An-Najah National University

Faculty of Graduate Studies

Magnetic properties of donor impurity in GaAs semiconductor quantum pseudo-dot system (GaAs)

By

Hanaa Mohammad Rehan

Supervisor

Prof. Mohammad Elsaid

This Thesis is Submitted in Partial Fulfillment of the Requirements for the Degree of Master in Physics, Faculty of Graduate Studies, An-Najah National University, Nablus - Palestine.

2019

Magnetic properties of donor impurity in GaAs semiconductor quantum pseudo-dot system

By

Hanaa Mohammad Rehan

This Thesis was Defended Successfully on …/…/2019 and approved by:

Defense Committee Members	**Signature**
1. Prof. Mohammad Elsaid (Supervisor)	**.....**
2. …… (External Examiner)	**.....**
3. …… (Internal Examiner)	**.....**

Dedication

For my husband and my children

For my mother and my father

For my brother and sisters.

Acknowledgements

I would like to thank Prof. Mohammad Elsaid who encouraged me to complete this thesis. I also thank him for his efforts, time and guidance, and I thank the Scientific Committee very much.

I do not forget the great thanks to Mr. Ayham Shaer for his efforts with us especially in Mathematica program.

الاقرار

انا الموقع ادناه مقدم الرسالة التي تحمل العنوان:

Magnetic properties of donor impurity in GaAs semiconductor quantum pseudo-dot system

أقر بأن ما اشتملت عليه هذه الرسالة انما هي نتاج جهدي الخاص، باستثناء ما تم الاشارة اليه حيثما ورد، وان هذه الرسالة ككل او اي جزء منها لم يقدم لينل اي درجة او لقب علمي او بحثي لدى اي مؤسسة تعليمية او بحثية اخرى.

Declaration

The work provided in this thesis, unless otherwise referenced, is the researcher's own work and has not been submitted elsewhere for any other degree or qualification.

الاسم: **Student Name:**

التوقيع: **Signature:**

التاريخ: **Date:**

Table of Contents

List of Tables

List of Figures

List of Abbreviations

QD	Quantum Dot
QW	Quantum Well
QWW	Quantum Well Wire
QPD	Quantum pseudo-dot
3D	Three Dimensions
2D	Two Dimensions
1D	One Dimension
0D	Zero Dimension
M	Magnetization
χ	Susceptibility
ω_c	Cyclotron Frequency
B	Magnetic field
F	Electric field
E	Charge of electron
m_0	Mass of electron (rest)
m*	Effective mass of electron
meV	milli electron Volt
nm	nano meter
k_B	Boltzman constant
P	Linear momentum
A	Vector potential
c	Speed of light
i	Imaginary number
T	Temperature
K	Kelvin degree
R*	Effective Rydberg energy unit
a*	Effective Bohr radius
ħ	Reduced Blank's constant
ε	Dielectric constant of material
L_z	the orbital angular momentum
$\bar{k}$	Shifted parameter
a	Shift parameter
m	Angular quantum number
l	Orbital quantum number
n_r	Radial quantum number
N	Dimension
ψ	Wave function

V_{eff}	Effective potential
$V_c(r)$	Confining potential
r	Position coordinate

Magnetic properties of donor impurity in GaAs semiconductor quantum pseudo-dot system

By

Hanaa Mohammad Rehan

Supervisor

Prof. Mohammad Elsaid

Abstract

The magnetic properties like magnetization and susceptibility of donor impurity in quantum pseudo-dot (QPD) are studied in the presence of the applied external magnetic and electric fields. The shifted 1/N expansion method has been used to solve the Hamiltonian of the donor impurity in (QPD). We calculate the energy eigenvalue for the ground state and low lying state as a function of magnetic field strength with various quantum dot physical parameters. Our computed energy results of the QPD show very good agreement compared with the corresponding reported work. These parameters are: the presence of the impurity, the electric field strength η, the magnetic field strength ω_c, the confinement pseud-dot potential: radius of QD (R_0) and the confinement strength (V_0). The dependencies of the binding energy and statistical energy on the electric field strength η, the magnetic field strength ω_c, and the confining pseud-dot potential (R_0 , V_0) are presented. Our results reveal that the presence of the impurity, the electric field strength η, the magnetic field strength ω_c, and the confinement pseud-dot potential (R_0 , V_0) have significant influences on magnetization and susceptibility. The magnetization and susceptibility

curves show oscillating behavior which is attributed to the energy level crossings of the QPD spectra.

Chapter One
Introduction

1.1 Quantum confinement effects

A quantum confined structure is one in which the motion of the carriers (electron and hole) are confined in one or more directions by potential barriers. Based on the confinement direction, the quantum confinement has significant effects on the physical properties of low-dimensional quantum system like: quantum well (QW), quantum wires (QWW), quantum dot (QD) and quantum pseudo-dot (QPD).

In quantum dot (0D), the charge carriers are confined in all three dimensions and electrons have discrete energy spectra. Quantum wires (1D), the charge carriers travel only along the wire direction (two dimensions of the system are confined). In quantum well (2D), charge carriers are confined to move in a plane and are free to move in two dimensional. Bulk materials do not show energy confinement effects.[1]

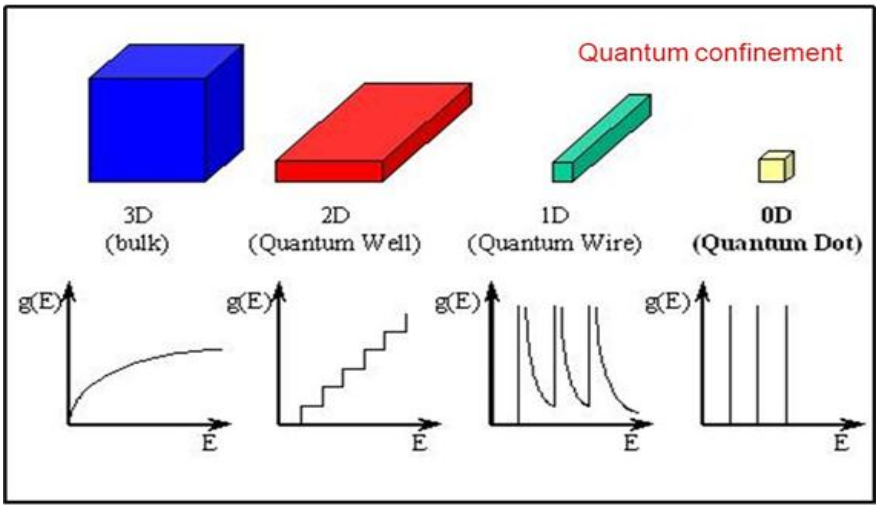

Figure (1.1): Density of electron states for low dimensional semiconductor systems [2].

1.2 Quantum Pseudo-dot

Quantum pseudo-dots (QPD) are nanoscale materials where the motion of the charge carriers have been limited in all dimensions. This carrier confinement leads to formation of discrete energy levels and the change of electronic and magnetic properties [3]. The nanoscale is defined from 1 to 100 nm.

The quantum pseudo-dot (QPD) consists of quantum dot and quantum anti-dot [4].

1.2.1 Quantum dots

Quantum dots (QDs) are nanostructure semiconductor materials closely confine either electrons or electron holes. Quantum dots are also sometimes referred to as artificial atoms. QD size ranges from 2-10 nanometers. So small that their optical and electronic properties differ from those of larger particles. Their size, shape and other properties can be controlled in experiment.

QDs is an important field of research for both pure and applied physics because of the large number of applications it has, such as: solar cells, diode lasers, transistors, medical imaging and quantum computing. These QDs materials have unique electronic properties [5].

1.2.2 Quantum Anti-dot

Anti-dots, in a moderate or high magnetic field, confined electrons to the edges of a sample, when external negative potential is applied at the center of the QPD, as shown in figure (1.2).

As the magnetic field or gate voltage is changed, the energy levels of the zero-dimensional states formed pass through the Fermi energy, causing the resistance to oscillate. The oscillations develop extra structure, such as double peaks. We can explain these effects in terms of transport through more than one of the edge states encircling the anti-dot [6].

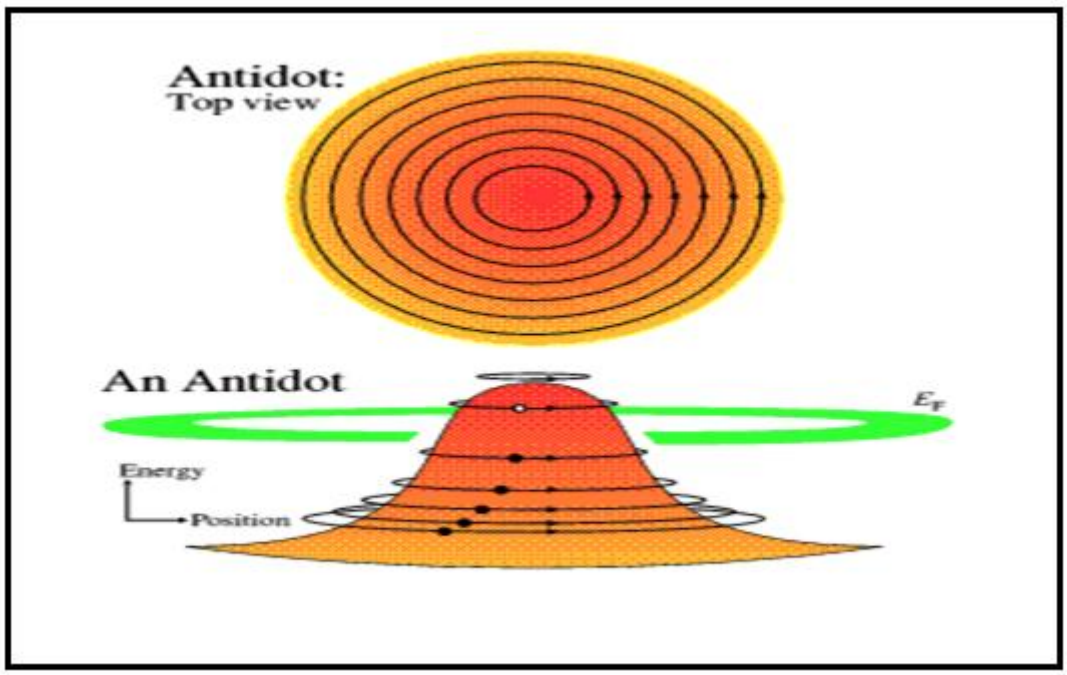

Figure (1.2): Edge states around an antidote[6].

The energy levels of the QPD can be controlled by applying external magnetic and electric fields, in addition to the impurities.

In our study, the heterostructures of QPD on the surface of a two-dimensional electron gas is formed by GaAs/AlGaAs layers, as shown in figure (1.3).

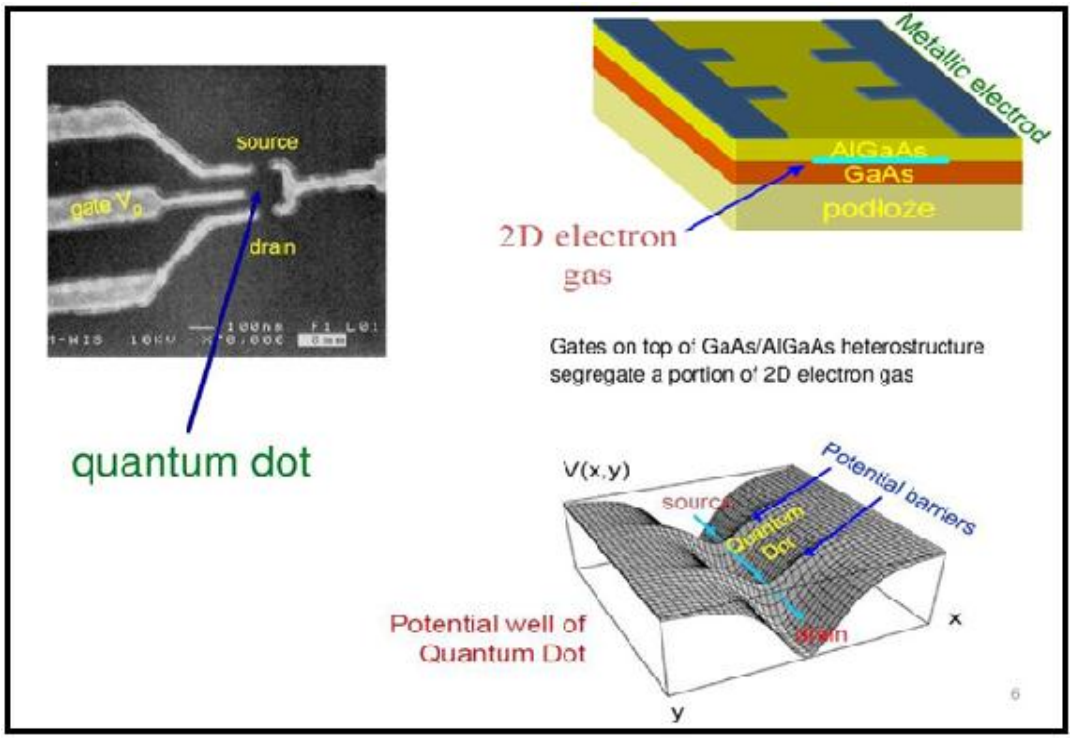

Figure (1.3): Quantum dot made from GaAs/ AlGaAs heterostructure in two dimensions[7].

The study of impurity in QPD has been of great interest to researchers, therefore a large number of theoretical works have been devoted to the understanding of confined impurity states in QPD system. Additionally, the external electric and magnetic fields are effective tools for investigating the properties of impurity in QPD.

In this thesis, we will study the effects of the electric and magnetic field on the energy spectra of donor impurity in QPD by using 1/N expansion method. The 1/N computational techniques will be used to solve the QPD Hamiltonian and obtain the eigenenergies of the donor impurity as a function of magnetic and electric fields.

1.3 Literature Survey

The effects of electric and magnetic fields on the impurity states in QPD have been studied recently. Different theoretical works had been devoted to solve the Schrodinger equation for this potential by using various methods such as: variational and perturbation method[8], asymptotic iteration method(AIM)[9]. R. Khordad [3,4] had studied three characteristics of a hydrogenic impurity located in the center of QPD within the effective mass approximation and the influence of Rashba effect on bound polaron in a QPD using the variational procedure. Dehyar and Zamani [10] studied the effects of the Kratzer potential on the hydrogenic impurity in external electric and magnetic fields by using AIM. G.Rezaei and Shojaeian [11] investigated the effects of electric and magnetic fields, pressure, temperature on the binding energy of hydrogenic donor impurity confined in 2D parabolic QD using the direct numerical diagonalization method. G.Rezaei and Doostimotlagh [12] used the direct numerical diagonalization to study the effects of conduction band non- parabolicity, electric field and pressure on the binding energy and magnetic susceptibility of hydrogenic donor impurity in QD. G.Rezaei, Taghizadeh

and Enshaeian [13] considered simultaneous effects of electric field, pressure, temperature on the binding energy of an off center hydrogenic donor confined by spherical Gaussian potential based on the effective mass approximation within a matrix diagonalization scheme. Jian and Chao [14] had computed of an off-center hydrogenic donor in a spherical QD with strong parabolic confinement by a perturbation method.

Aydogdu and Sever [15] had used the Nikiforov – Uvarov method to compute the energy spectra and corresponding wave functions of the Dirac equation for pseudo harmonic potential. R.Khordad [16] had calculated the electronic and optical properties in QD with Kratzer potential by using the numerical diagonalization method. Investigation of magnetic field effects on binding energies in spherical QD with finite confinement potential had been carried by Bekir Çakır, Yusuf Yakar, Ayhan Ozmen [17]. While D.B. Hayrapetyan, S.M. Amirkhanyan, E.M. Kazaryan, H.A. Sarkisyan [18] had studied the effects of hydrostatic pressure on diamagnetic susceptibility of hydrogenic donor impurity in spherical QD with Kratzer confining potential. D.Sanjeev Kumar, Soma Mukhopadhyay, Ashok Chatterjee [19] had studied the magnetization and susceptibility of a two-electron parabolic QD in the presence of electron–electron and spin–orbit interactions as a function of magnetic field and temperature. M. Akbari G. Rezaei R. Khordad [20] had considered the impact of the spin-orbit coupling on the level structure in 2D-QPD. Elsaid et.al. [21-30] had also investigated , very recently , the magnetic properties of two-interacting electrons in a single and double QDs, which are presented in a magnetic field. The

energy spectrum, the optical and electromagnetic properties of a donor impurity confined by 2D of an electron confined by a pseudoharmonic potential in the presence of a strong magnetic field are investigated [31-34].

In this work, we use the shifted 1/N expansion method to calculate the eigenenergies of donor impurity in a QPD under the effects of the electric and magnetic fields. The obtained eigenenergies will be used as input data to compute the average statistical energy, magnetization and magnetic susceptibility of the impurity in QPD system made from GaAs material.

1.4 Research Objectives

This research has two objectives which can be summarized as follows:

Firstly, QPD Hamiltonian will be solved by using 1/N expansion method to obtain the eigenenergies of the donor impurity in QPD in different ranges of electric and magnetic field strengths.

Secondly, the magnetization and magnetic susceptibility of donor impurity in QPD will be studied as function of the physical parameters of the QPD system: strengths of magnetic (ω_c), electric fields (η) and the confining potential (V_0 , R_0).

Chapter Two
Theory

This chapter consists of three main parts:

i) The Hamiltonian of donor impurity in 2D QPD under the effects of electric and magnetic field.

ii) 1/N shifted expansions method.

iii) the magnetic properties of QPD: magnetization and magnetic susceptibility.

2.1 QD Hamiltonian

The Hamiltonian of donor impurity confined in 2D QPD under the influence of external electric and magnetic fields, can be written as:

$$H = \frac{1}{2m^*}\left(\vec{P} + \frac{e}{c}\vec{A}\right)^2 - \frac{e^2}{\varepsilon r} - e\eta r + V(r) \qquad (2.1)$$

Where $\vec{A}$ is a vector potential, given by: $\vec{A} = \frac{1}{2} B \times \vec{r}$

ε is the dielectric constant of the medium (GaAs),

c is the speed of light, e is the electron charge,

$\vec{P}$ is the electron momentum operator, given by: $\vec{P} = \frac{-\hbar}{i}\nabla$

η is the strength of the electric field.

m* is the effective mass of the electron in GaAs material that equals $0.067m_e$

$-\frac{e^2}{\varepsilon r}$ represents the coulomb attractive energy between the electron and the donor impurity center.

r is the electron position coordinate r = (x,y) from the center of the QD in a 2D.

V(r) is the pseudo harmonic confining potential that includes both harmonic QD potential and anti-dot potential [4],

$$V_c(r) = V_0\left(\frac{r}{R_o} - \frac{R_o}{r}\right)^2 \qquad (2.2)$$

V_0 is the strength of the potential.

R_0 is the zero point of the pseudo-dot harmonic potential.

The potential can be rewritten as:

$$V_c(r) = \frac{A}{R_0^2} + BR_0^2 - 2V_0$$

This model can also be applied to describe of several other physical systems:

When $R_0 \to \infty$,the system becomes straight wires. If we take $A = 0$, the QPD becomes the parabolic confinement potential for QD $V_c(r) = BR_0^2$. When $B = 0$, the potential becomes $V_c(r) = \frac{A}{R_0^2}$, which describe an anti-dot [35].

It is important to note that the QPD systems with $V_c(r)$ potential can be solved analytically in 1D, 2D and 3D [36].

The Hamiltonian of this system Eq (2.1), using the symmetric gauge $\vec{A} = \frac{B}{2}$ (-y,x,0) , is given by:

$$H = -\frac{\hbar^2}{2m^*}\nabla^2 + \frac{1}{8}m^*\omega_c^2 r^2 + \frac{1}{2}\omega_c L_z - \frac{e^2}{\epsilon r} - e\eta r + V_c(r) \qquad (2.3)$$

Where L_z is the orbital angular momentum, $\omega_c = \frac{eB\hbar}{2m^* R^*} = 0.308 * B(T)$ is the magnetic field cyclotron frequency, $\eta = \frac{e\alpha^* F}{R^*} = 0.179 * F(\frac{kV}{cm})$ is the electric field strength in units of R*. We use ħ=1, ε=1, e=$\sqrt{2}$.

In this work, we use the effective Rydberg units $R^* = \frac{m^* e^4}{2\epsilon^2\hbar^2}$ =5.61meV, and Bohr radius $\alpha^* = \frac{\epsilon\hbar^2}{m^* e^2}$ = 10.04nm, for GaAs material.

It is clear that the Hamiltonian of the QPD given by Eq (2.1) is quite complex and cannot be solved analytically. In this work we will implement the shifted 1/N expansion method to solve the Eq (2.3) to obtain the desired energies which in turn be used to study M, χ of an electron in QPD.

2.2 The Shifted 1/N Expansion method

The shifted 1/N expansion method has been used to solve the Schrodinger equation for N-dimensions. It gives exact results for Harmonic oscillator and Coulomb potentials. This method is quite simple technique and ensures high accuracy. The radial part of Schrodinger equation in an N dimensional space is [37] :

$$\left\{\frac{-\hbar^2}{2m}\left(\frac{d^2}{dr^2}+\frac{N-1}{r}\frac{d}{dr}\right)+\frac{l(l+N-2)\hbar^2}{2mr^2}+V(r)\right\}\psi=\mathrm{E}\psi \qquad (2.4)$$

Where $V(r)$ is the effective potential of Eq (2.3) given as:

$$V_{eff}(r)=\frac{1}{8}m^*\omega_c^2r^2+\frac{1}{2}\omega_cL_z-\frac{e^2}{\in r}-\mathrm{e\eta r}+V_0\left(\frac{r}{R_o}-\frac{R_o}{r}\right)^2 \qquad (2.5)$$

The term: $l(l+N-2)\hbar^2$ is the eigenvalue of the square of the orbital angular momentum operator in N dimensional space and $l=|m_l|$ where m is the magnetic quantum number $m=(0,\pm1,\pm2,\ldots..)$ in 2D space.

The main concept of 1/N expansion method is to rewrite Eq (2.4) by using a parameter as $k=N+2l$ and shift parameter a. We use $\bar{k}$ which is defined $\bar{k}=k-a$ and Eq (2.1) takes the form:

$$\left\{-\frac{\hbar^2}{2m}\frac{d^2}{dr^2}+\bar{k}\left[\frac{\hbar^2(1-(1-a)/\bar{k})(1-(3-a)/\bar{k})}{8mr^2}+\frac{V(r)}{Q}\right]\right\}\psi=E\psi \qquad (2.6)$$

Where Q is a scaling constant, chosen to make Eq (2.4) and (2.6) equals, this means; $\bar{k}=\sqrt{Q}$

For large $\bar{k}$, the energy comes from the effective potential and the kinetic energy becomes negligible. The effective potential V_{eff} reads as:

$$V_{eff}=\frac{\hbar^2}{8mr^2}+\frac{V(r)}{Q} \qquad (2.7)$$

$V(r)$ is assumed to be well behaved so that V_{eff} has minimum at $r=r_0$ given by the form:

$$4mr_0^3V`(r_0)=\hbar^2Q \qquad (2.8)$$

Shifting the origin r_0 to the position of the minimum of the effective potential (x=0) by a new variable as:

$$x = \frac{\sqrt{\bar{k}\cdot}}{r_0}(r - r_0) \tag{2.9}$$

By using Taylor expansion of the Schrodinger equation around the effective potential minimum $x = 0$,

The energy eigenvalues are given:

$$E(n, l) = E_0 + E_1 + E_2 + \ldots\ldots \tag{2.10}$$

The shift parameter a can be determined by taking $(E_1 = 0)$ so:

$$a = 2 - 2(2n_r + 1)\frac{m^*\omega}{\hbar} \tag{2.11}$$

Where ω is defined as an oscillator potential with frequency:

$$\omega = \frac{\hbar}{2m}\left(3 + \frac{r_0 V``(r_0)}{V`(r_0)}\right)^{1/2} \tag{2.12}$$

The root r_0 is determined from Eq (2.8), (2.11) and (2.12) by the relation:

$$\left(\frac{4m_0 r_0^3 V`(r_0)}{\hbar^2}\right)^{1/2} = N + 2l - 2 + (2n_r + 1)\left(3 + \frac{r_0 V``(r_0)}{V`(r_0)}\right)^{1/2} \tag{2.13}$$

After determining the roots (r_0), the eigenenergies can be computed for any quantum state: $|n_r,m>$ with different ranges of external fields and confining potential parameters. The energy expression is very long to be repeated here. The complete eigenvalue equations are given, in terms of quantum

numbers, an harmonic frequency and potential derivatives, the interested reader can refer to [38].

2.3 Magnetization of QPD (M)

The magnetization is one measure of the magnetic properties of a material, it can be calculated from the statistical energy according to the following relation:

$$M(\omega_c, \eta, R_0, V_0) = -\frac{\partial <E>}{\partial B} \quad (2.14)$$

Where the statistical energy is given as:

$$< E > = \sum_{\alpha=1}^{i} \frac{E_\alpha e^{-E_\alpha / k_B T}}{\sum_{\alpha=1}^{i} e^{-E_\alpha / k_B T}} \quad (2.15)$$

Where α indicates the quantum states of the QPD represented by the Hamiltonian given in Eq (2.1) and k_B is the Boltzman constant .

2.4 The magnetic susceptibility of QPD (χ)

Another important physical quantity is the magnetic susceptibility (χ), if χ is positive a material can be classified as paramagnetic. if χ is negative, the material is diamagnetic. χ is defined as the variation of the magnetization of the QPD systems as we vary the magnetic field, B. as:

$$\chi = \frac{\partial M}{\partial B} \quad (2.16)$$

Chapter Three

Results and Discussions

This chapter is devoted for computed numerical results of the electronic and magnetic properties of QDs (energies, binding energies, magnetization and magnetic susceptibility). The analysis of these obtained results are also presented.

3.1 Energy spectra

In the first step in our work, we have calculated the energy spectrum without impurity of GaAs QPD at different values of magnetic and electric fields. It is important to mention that the energy expression of the QPD-Hamiltonian, in special cases like zero electric field and no impurity, can be obtained in a closed analytic form [Ref.20]. Thus, we use in this work the shifted 1/N expansion method to solve the full QPD Hamiltonians including all external potential terms.

In figure (3.1), we have plotted the energy spectrum for ground and exited states as a function of magnetic field strength without impurity and zero electric field, we compare our figure (3.1.a) with figure (3.1.b) of Ref [20]. The comparison shows good agreement between both results.

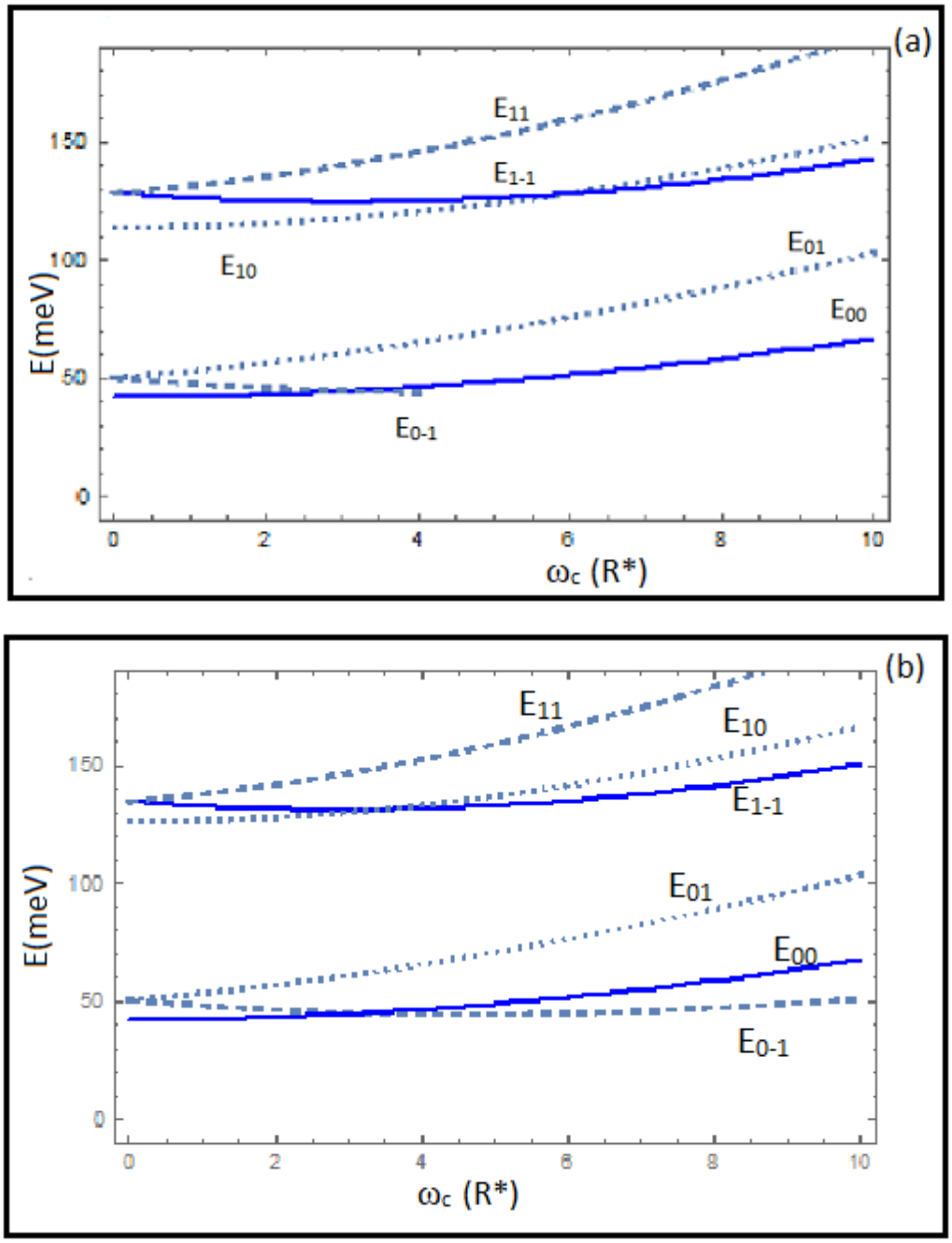

Figure (3.1): The energy spectrum versus magnetic field calculated at R_0=8nm, V_0=50meV and zero electric field without impurity, a)Present work, b)Ref [20].

To see the effects of magnetic and electric fields, confinement and impurity on the energy spectra of QPD. Figure (3.2) shows the enhancement of the QPD energy of the electron as the magnetic field increases. The presence of

the impurity decreases the energy of the electron due to the attractive energy contribution in QPD.

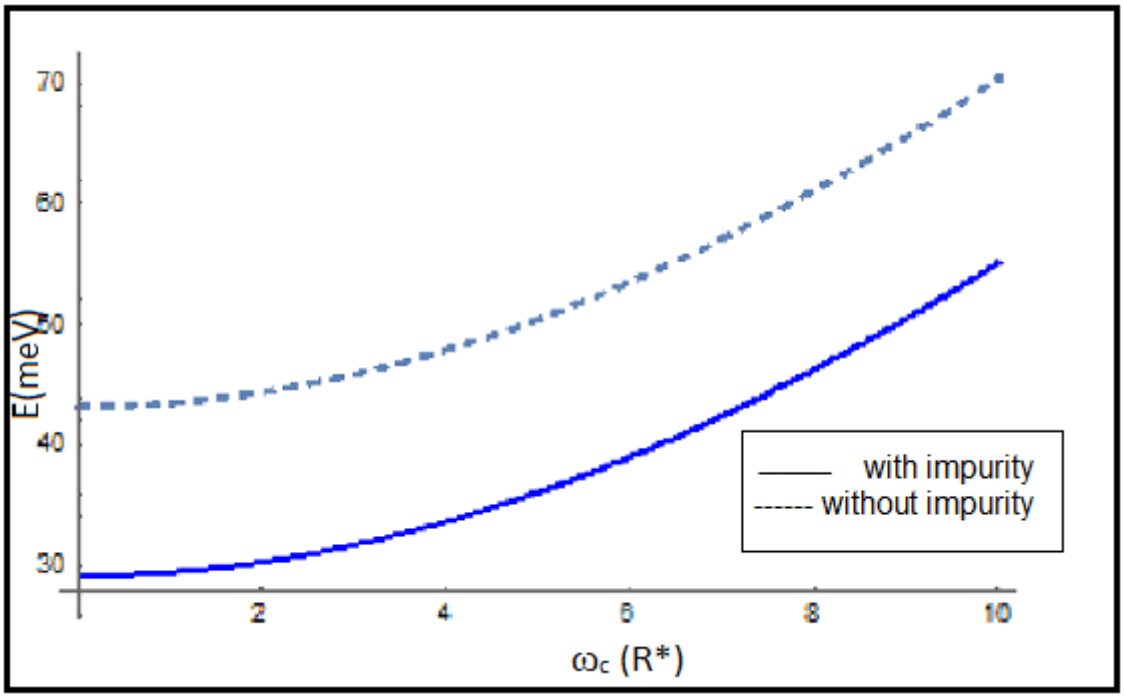

Figure (3.2): The ground state energy as a functions of magnetic field ω_c with (solid line)/without (dashed line) impurity, at R_0=8nm, V_0=50meV for zero electric field η=0R*.

In figure (3.3) and (3.4), we have shown the effects of the electric field on the energy of the electron with and without donor impurity. The figures show a significant reduction in the energy of the confined electron in the QPD. This energy reduction is due to the attractive coulomb energy since the electric field displaces the electron far away from the donor impurity.

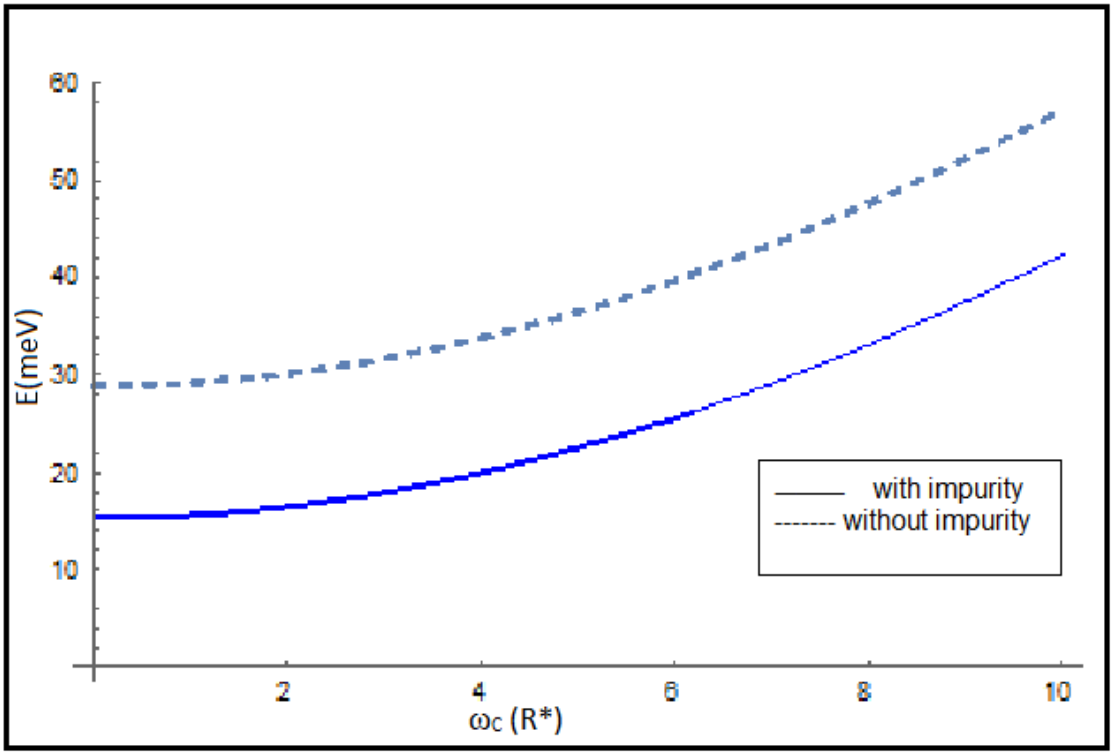

Figure (3.3): The ground state energy as a functions of magnetic field ω_c with (solid line)/without (dashed line) impurity, at R_0=8nm, V_0=50meV and η=2R*.

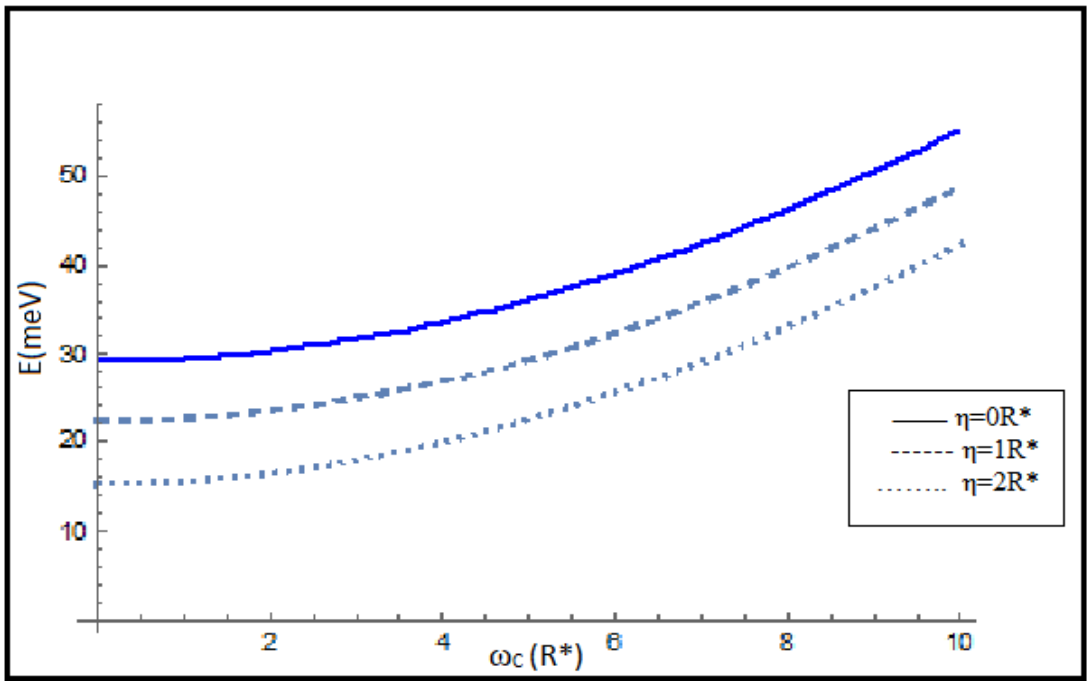

Figure (3.4): The ground state energy as a functions of magnetic field ω_c at V_0=50meV, R_0=8nm for different values of η.

Figure (3.5) shows the effects of the confinement V_0 on the electron energy spectra. As the confinement strength V_0 increases (from 20 to 50 meV), this leads to stronger confinement potential of the electron which enhances the electron energy in QD. In figure (3.6) we have shown the effects of the QD zero point R_0 increases. As R_0 decreases the electron becomes more confined and thus the energy enhanced. Whereas, at very strong magnetic field (ω_c = 8.5R*) as shown in table (3.1), the energy increases as the zero point R_0 increases.

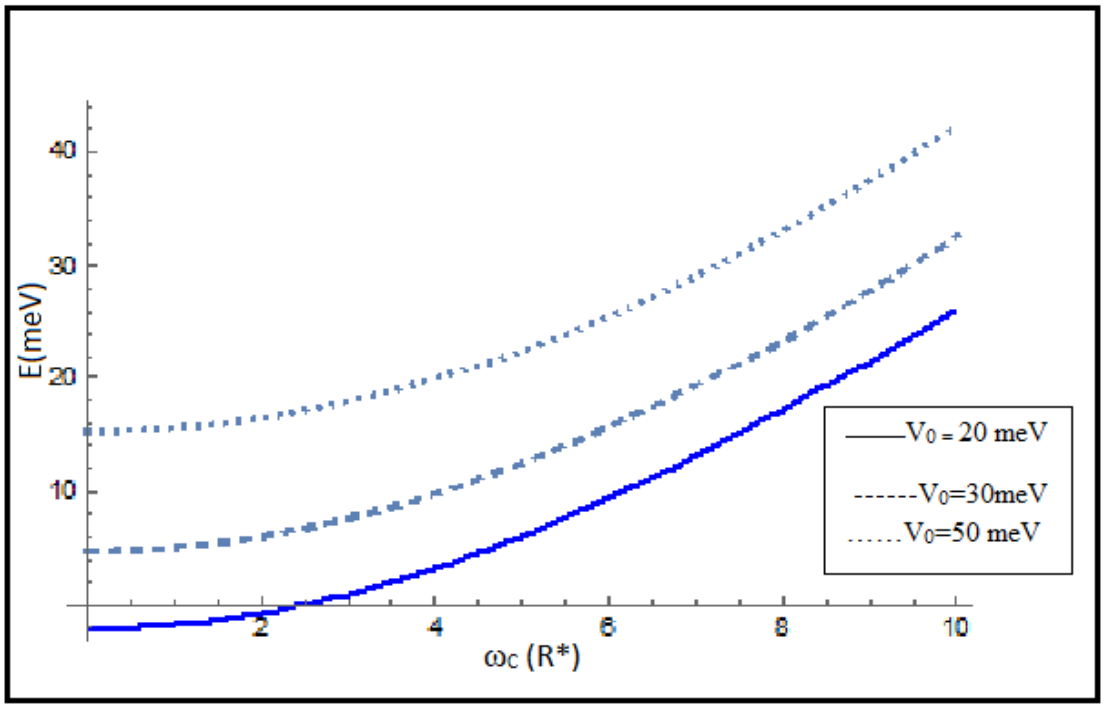

Figure (3.5): The ground state energy as a functions of magnetic field ω_c , at R_0=8nm, η=2R* for different values of V_0 .

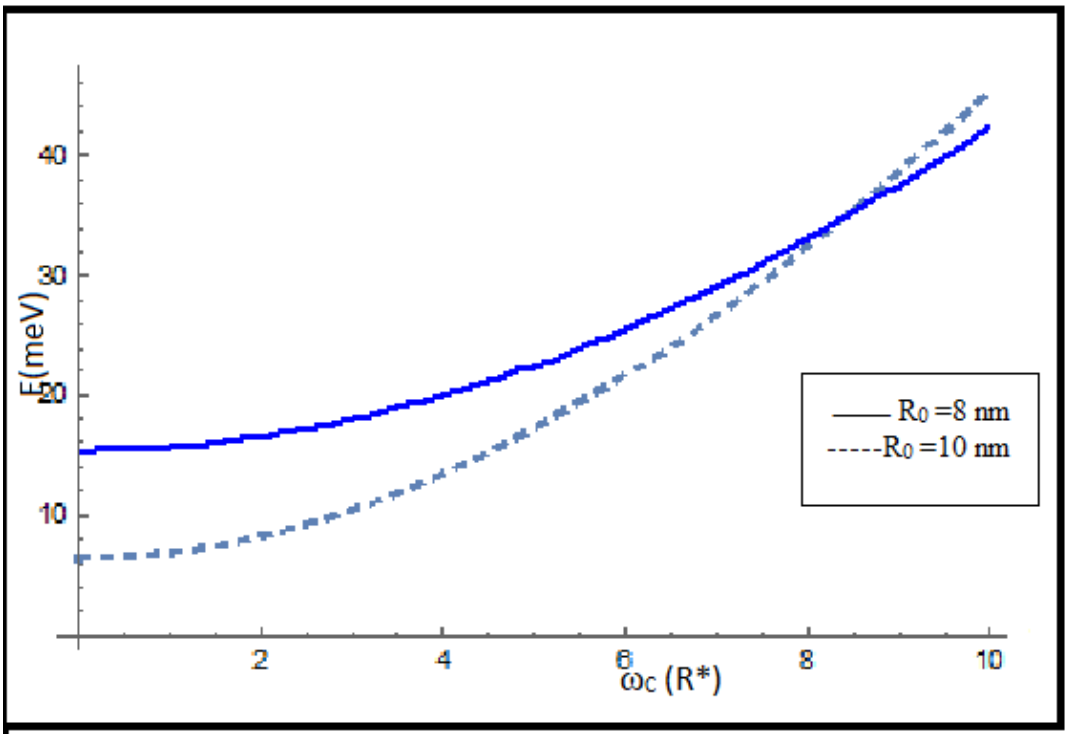

Figure (3.6): The ground state energy as a functions of magnetic field ω_c , at V_0=50meV, η=2R* for different values of R_0.

Table (3.1):. The ground state energy as a functions of magnetic field ω_c , at V_0=50 meV, η=2R* for different values of R_0.

E(meV)		ω_c(R*)
R_0 =8 nm	R_0 = 10 nm	
28.5785	26.6617	7.0
30.6364	29.5924	7.5
32.8059	32.6634	8.0
35.0821	**35.8665**	**8.5**
37.4606	39.1937	9.0
39.9367	42.6376	9.5
42.5061	46.1907	10

In figure (3.7), we have shown the energy against the magnetic field strength for electric field strength η=2R*. The plot shows the energy splitting for positive and negative angular momenta values, due to the

magnetic field effect. The computed eigenenergies of the QDs against the magnetic field are also listed in table (3.2) .

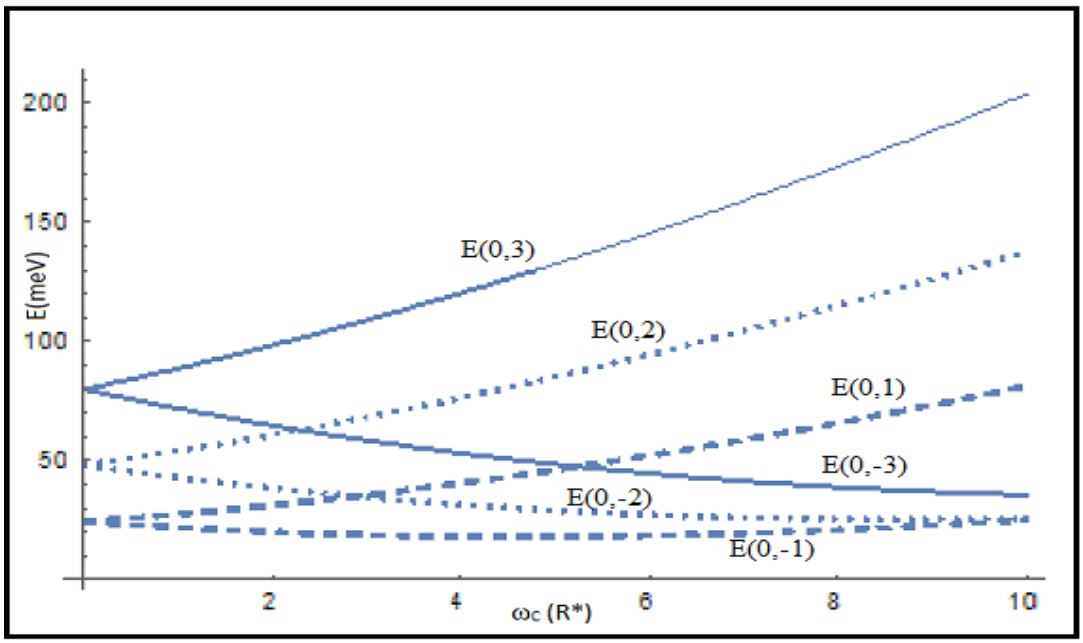

Figure (3.7): The energy for low lying excited states of the donor impurity as a function of the magnetic field strength ω_c calculated at R_0=8nm, V_0=50meV and η=2R*.

In table (3.2) we computed the energy spectra with magnetic field strength ω_c , at R_0=8nm, V_0=50meV and zero electric field (η=0R*), without impurity, and plotted the results in figure (3.8). We note that the state of E (0,-1) crossing with the ground state at ω_c=3R*, the state of E (0,-2) crosses with the ground state aT ω_c=6R*, the state of E (0,-3) crosses with the ground state at ω_c= 8.5R*, and the state of E (0,-4) crosses with the ground state at ω_c= 10.5R*.

Table(3.2): The energy spectra and the level crossings versus magnetic field strength ω_c calculated at R_0=8nm, V_0=50meV and zero electric field η=0R*, without impurity.

ω_c (R*)	E(0,0) (meV)	E(0,-1) (meV)	E(0,-2) (meV)	E(0,-3) (meV)	E(0,-4) (meV)
0.0	41.7759	50.1035	72.5068	102.918	137.649
0.5	41.8548	48.7845	69.7978	98.8230	132.171
1.0	42.0911	47.6322	67.2804	94.9539	126.957
1.5	42.4842	46.6459	64.9537	91.3090	122.006
2.0	43.0328	45.8242	62.8162	87.8866	117.316
2.5	43.7349	45.1651	60.8655	84.6841	112.883
3.0	**44.5885**	**44.6663**	59.0991	81.6982	108.703
3.5	45.5908	44.3250	57.5137	78.9253	104.774
4.0	46.7389	44.1380	56.1056	76.3609	101.088
4.5	48.0292	44.1016	54.8706	74.0002	97.6407
5.0	49.4581	44.2119	53.8043	71.8379	94.4260
5.5	51.0218	44.4649	52.9018	69.8684	91.4370
6.0	**52.7159**	44.8561	**52.1582**	68.0857	88.6668
6.5	54.5364	45.3810	51.5682	66.4837	86.1083
7.0	56.4786	46.0348	51.1265	65.0561	83.7540
7.5	58.5383	46.8130	50.8276	63.7965	81.5964
8.0	60.7108	47.7106	50.6660	62.6984	79.6281
8.5	**62.9917**	48.7229	50.6363	**61.7554**	77.8413
9.0	65.3764	49.8452	50.7329	60.9610	76.2286
9.5	67.8605	51.0728	50.9505	60.3090	74.7826
10.0	70.4398	52.4010	51.2838	59.7930	73.4960
10.5	**73.1099**	53.8254	51.7277	59.4071	**72.3617**
11.0	75.8666	55.3417	52.2770	59.1453	71.3727
11.5	78.7061	56.9454	52.9270	59.0018	70.5223
12.0	81.6244	58.6326	53.6728	58.9711	69.8040
12.5	84.6178	60.3993	54.5100	59.0478	69.2116
13.0	87.6826	62.2416	55.4341	59.2269	68.7389
13.5	90.8155	64.1560	56.4411	59.5033	68.3803
14.0	94.0131	66.1389	57.5268	59.8724	68.1303
14.5	97.2723	68.1871	58.6875	60.3297	67.9834
15.0	100.590	70.2973	59.9194	60.8708	67.9348

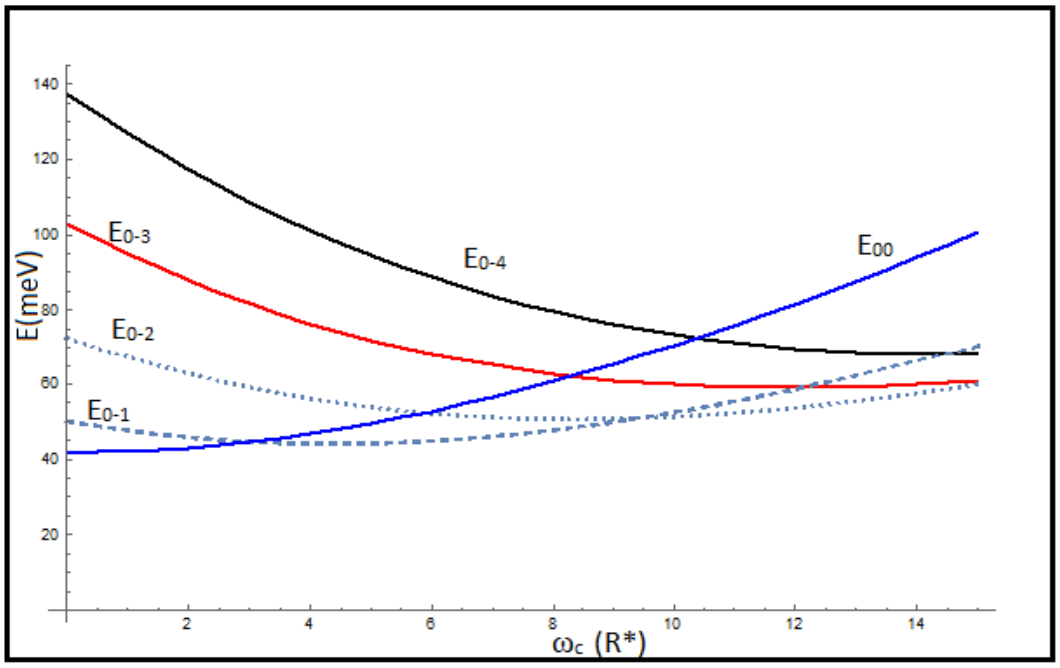

Figure (3.8): The energy and the level crossings for low lying excited states as a function of the magnetic field strength ω_c , at R_0=8nm, V_0=50meV and η=0R*, without impurity.

In table (3.3) we computed the energy spectra with magnetic field strength ω_c , at R_0=8nm, V_0=50meV and η=2R*, with impurity, and plotted this in figure (3.9), The figure clearly shows the energy level crossing at different values of magnetic field strength. For example, the state of E (0,-1) crosses the ground state at ω_c=3R*; the state of E (0,-2) crosses the ground state at ω_c=6R*; the state of E (0,-3) crosses the ground state at ω_c= 8.5R*; and the state of E (0,-4) crosses the ground state at ω_c= 10.5R*.

Table (3.3): The energy spectra and the level crossings versus magnetic field strength ω_c , at R_0=8nm, V_0=50meV and η=2R*, with impurity.

ω_c (R*)	E(0,0) (meV)	E(0,-1) (meV)	E(0,-2) (meV)	E(0,-3) (meV)	E(0,-4) (meV)
0.0	13.8481	22.2096	44.5316	74.5881	108.734
0.5	13.9274	20.8913	41.8239	70.4955	103.259
1.0	14.1648	19.7408	39.3102	66.6322	98.0534
1.5	14.5596	18.7574	36.9896	62.9971	93.1156
2.0	15.1104	17.9397	34.8604	59.5881	88.4434
2.5	15.8153	17.2855	32.9203	56.4026	84.0336
3.0	**16.6270**	**16.7924**	31.1664	53.4370	79.8821
3.5	17.6776	16.4574	29.5953	50.6875	75.9843
4.0	18.8289	16.2771	28.2029	48.1492	72.3347
4.5	20.1223	16.2477	26.9849	45.8170	68.9272
5.0	21,5540	16.3651	25.9367	43.6853	65.7552
5.5	23.1199	16.6249	25.0530	41.7482	62.8117
6.0	**24.8156**	17.0226	**24.3286**	39.9993	60.0894
6.5	26.6366	17.5533	23.7581	38.4323	57.5807
7.0	28.5785	18.2123	23.3358	37.0404	55.2777
7.5	30.6364	18.9945	23.0559	35.8169	53.1727
8.0	32.8059	19.8951	22.9128	34.7551	51.2576
8.5	**35.0821**	20.9090	22.9008	**33.8481**	49.5245
9.0	37.4606	22.0315	23.0142	33.0895	47.9656
9.5	39.9367	23.2576	23.2474	32.4724	46.5732
10.0	42.5061	24.5828	23.5951	31.9906	45.3396
10.5	**45.1644**	26.0023	24.0518	31.6377	**44.2576**
11.0	47.9074	27.5118	24.6124	31.4076	43.3199
11.5	50.7311	29.1069	25.2719	31.2945	42.5197
12.0	53.6315	30.7834	26.0256	31.2926	41.8503
12.5	56.6050	32.5375	26.8688	31.3966	41.3051
13.0	59.6478	34.3651	27.7971	31.6011	40.8782
13.5	62.7566	36.2628	28.8063	31.9011	40.5636
14.0	65.9281	38.2270	29.8922	32.2919	40.3556
14.5	69.1591	40.2544	31.0512	32.769	40.2491
15.0	72.4467	42.3418	32.2794	33.3279	40.2387

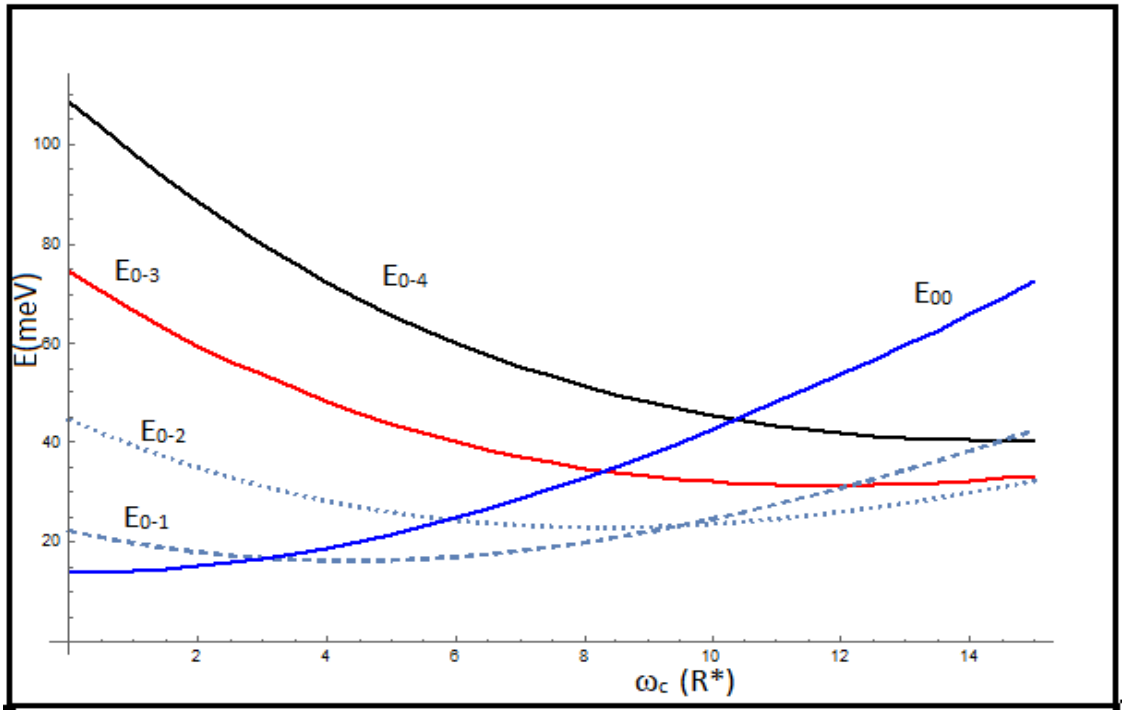

Figure (3.9): The energy level crossing for low lying excited states of the donor impurity as a function of the magnetic field strength ω_c , at R_0=8nm, V_0=50meV and η=2R*.

By comparison figure (3.8) with figure (3.9), it is clear that the presence of the impurity and the electric field decreases the energy state and the crossing of the state energy with the ground state energy at the same points of the magnetic field strength ω_c regardless of the donor impurity and the electric field. The crossing levels of the energy explains the oscillator in the figure of the statistical energy with magnetic field strength ω_c in section 3.3.

3.2 Binding energy

In this section we will present our computed results for the binding energy of donor impurity in QPD with different physical parameters.

The donor binding energy (B.E) is defined as the energy difference of the Hamiltonian without and with donor impurity,

$$B.E = \langle H \rangle_{impurity=0} - \langle H \rangle_{impurity=1} \quad (3.1)$$

In figure (3.10), we have shown the effects of the magnetic and electric fields on the binding energy of donor impurity of the electron confined in QPD. As the strength of the electric field increases, the binding energy decreases, as expected and explained previously in figure (3.4). The binding energy enhances as the magnetic field strength becomes stronger. This is because the increasing of the electric field causes the electron to be less confined to the impurity so it reduces the binding energy. In addition, the magnetic field increases the confinement of electron which in turn leads to increasing the binding energy. We note that at high magnetic field the effects of the electric field on the binding energy is small, as shown in table (3.4).

Table (3.4): The binding energy verses the magnetic field strength ω_c calculated at R_0 =8nm, V_0 =50meV, for different values of electric field strength η.

B.E (meV)			ω_C (R*)
η =0R*	η =2R*	η =5R*	
0.24952	0.23512	0.21213	0
0.26744	0.25497	0.23527	2
0.30659	0.29717	0.28253	4
0.35016	0.34298	0.33194	6
0.39241	0.38671	0.37801	8
0.43212	0.42743	0.42029	10

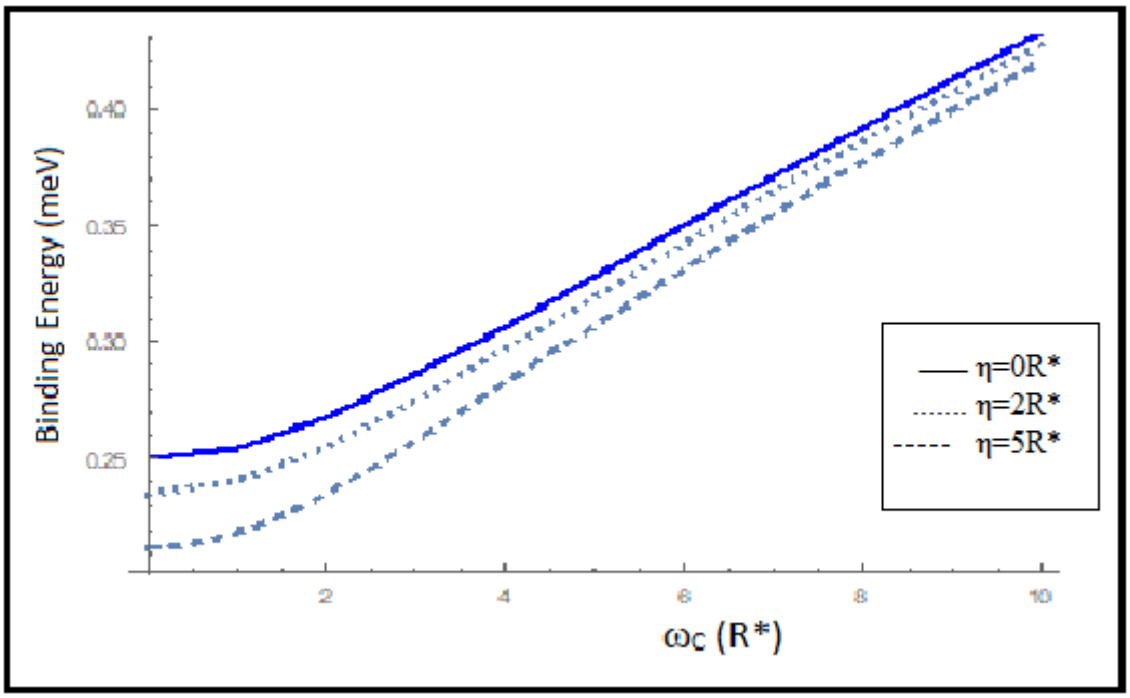

Figure(3.10): The binding energy for ground state of the donor impurity as a function of magnetic field strength ω_c, calculated at: V_0=50mev, R_0=8nm for various values of electric field η.

Figure (3.11) shows the dependence of the binding energy against the magnetic field strength for various R_0 , as the R_0 decreases, the donor binding energy increases. This is due to the fact that as the value of R_0 increases the binding of the electron to the donor impurity parent decreases.

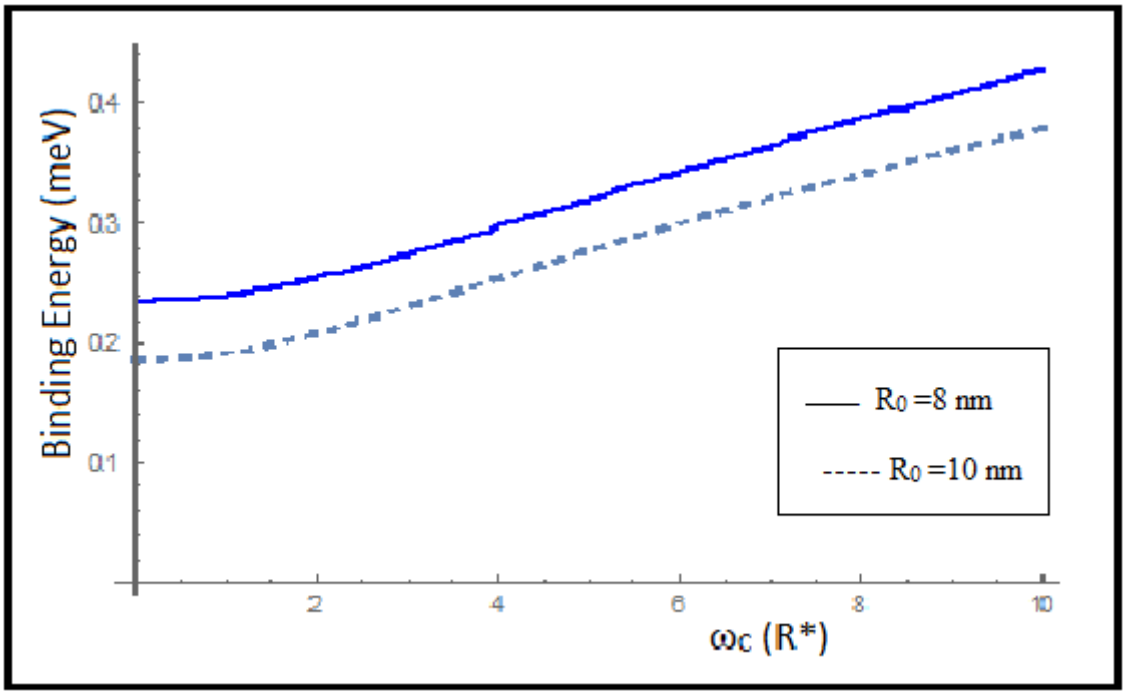

Figure (3.11): The binding energy for ground state of the donor impurity as a function of magnetic field strength ω_c for $\eta=2R^*$ and $V_0=50$ meV, for different values R_0 .

We show the variation of donor binding energy with the confinement potential V_0 in figure (3.12). By increasing the potential confinement V_0 the electron becomes more confined and therefore the binding energy increases. While, at middle and high magnetic field strengths, the binding energy decreases as we increase the potential strength V_0 . The data shown in table (3.5), at $\omega_c = 1.7$ R * reflects also the relation between the binding energy and the potential strength V_0 .

Table (3.5): The binding energy versus the magnetic field strength ω_c calculated at R_0 =8nm, η=2R*, for different values of V_0.

B.E (meV)			ω_C (R*)
V_0=10meV	V_0=30meV	V_0=50meV	
0.1721	0.22504	0.2351	0.0
0.1819	0.2275	0.2365	0.5
0.2067	0.2345	0.2405	1.0
0.23808	0.2451	0.2468	1.5
0.25108	**0.25006**	**0.2499**	**1.7**
0.26403	0.25534	0.2532	1.9
0.2704	0.25808	0.2549	2.0
0.2831	0.2637	0.25863	2.2

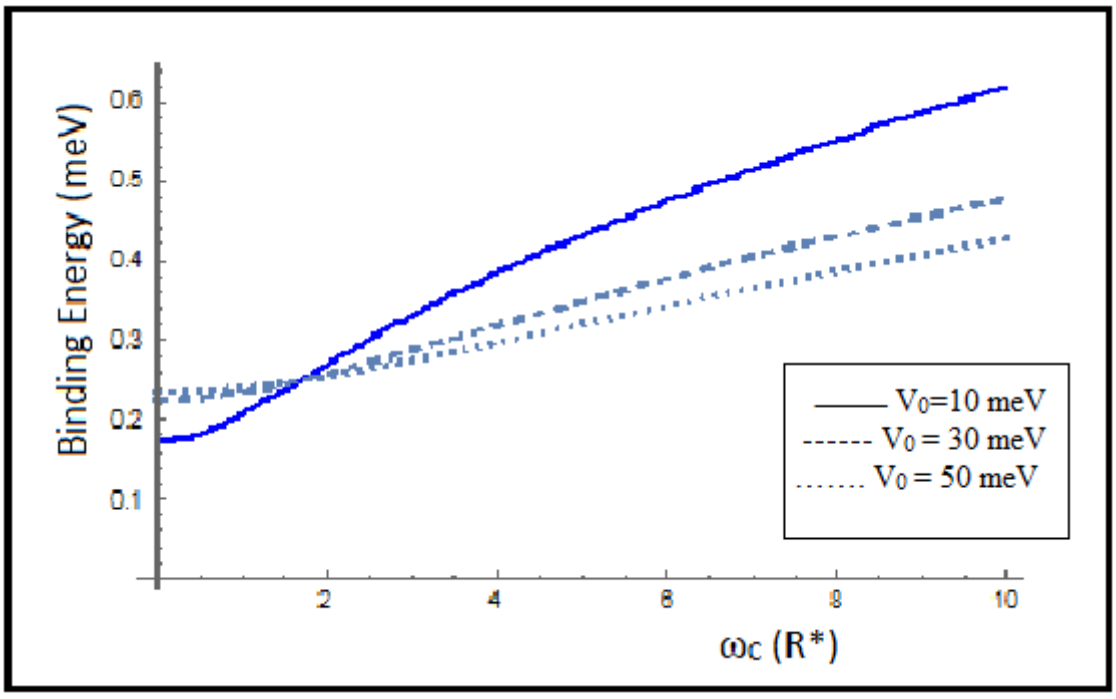

Figure (3.12): The binding energy for the ground state of the donor impurity as a function of magnetic field strength ω_c, at η=2R* and R_0=8 nm, for different values V_0.

3.3 Statistical energy

To ensure the accuracy of the presented computed results, we vary the number of states, until we achieve the numerical stability in the statistical energy of the QPD, as shown in figures (3.13), (3.14) and (3.15). Figures (3.13.a) and (3.13.b) show the statistical energy as a function of the magnetic field strength calculated at zero electric field with different quantum states. These figures show that the number of states has no effects on the statistical energy.

In figure (3.14), we test the convergency issue of the computed data for finite electric field strength $\eta = 2R^*$. We achieve again a very good convergency behavior in the computed statistical energy calculations.

In figure (3.15), show the statistical energy as a function of the magnetic field strength as we decrease the potential strength V_0 from 50 meV to 30 meV, with vary the number of state, the statistical energy as a function of the magnetic field decreases due to reduction of the potential strength V_0. We achieve again that the number of states has no effects on the statistical energy.

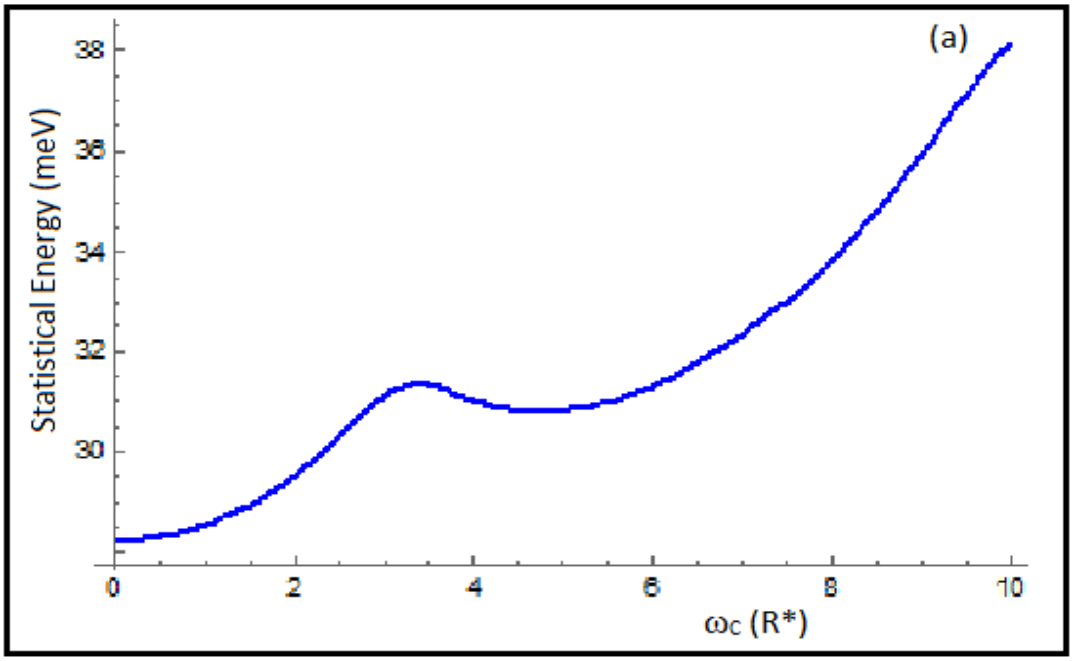

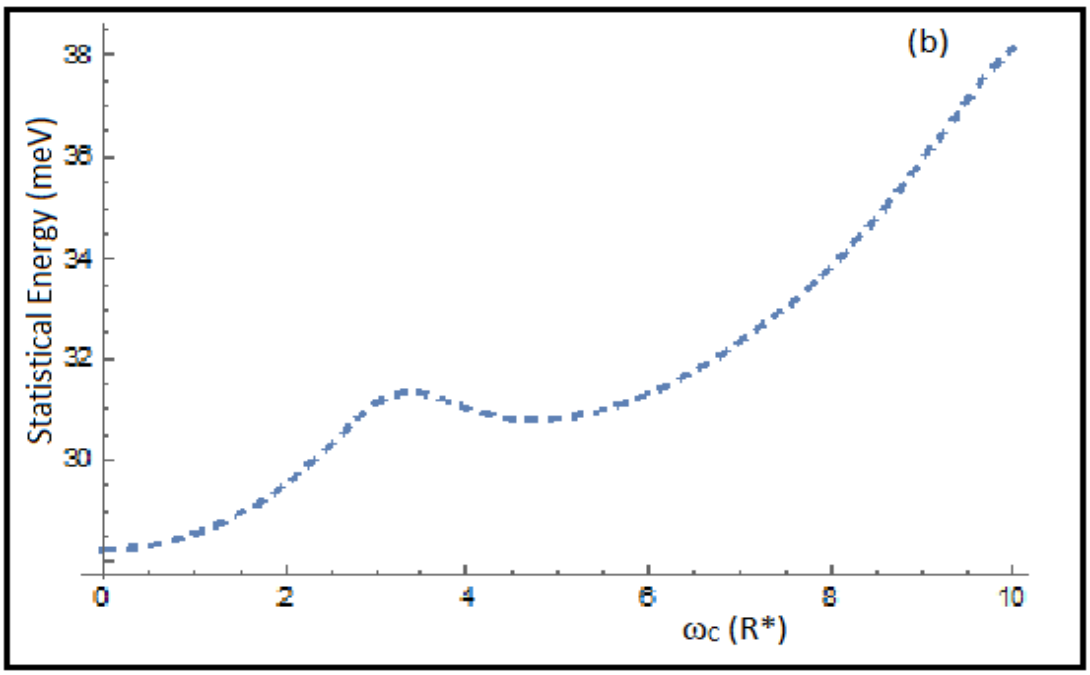

Figure(3.13): The statistical energy as a function of the magnetic field strength ω_c , at: η=0R*, V_0=50 meV, T=10 K, R_0 =8 nm, for different quantum number. a) The radial quantum number n (0,2) and the angular quantum number m (-2,2). b) The radial quantum number n (0,4) and the angular quantum number m (-4,4).

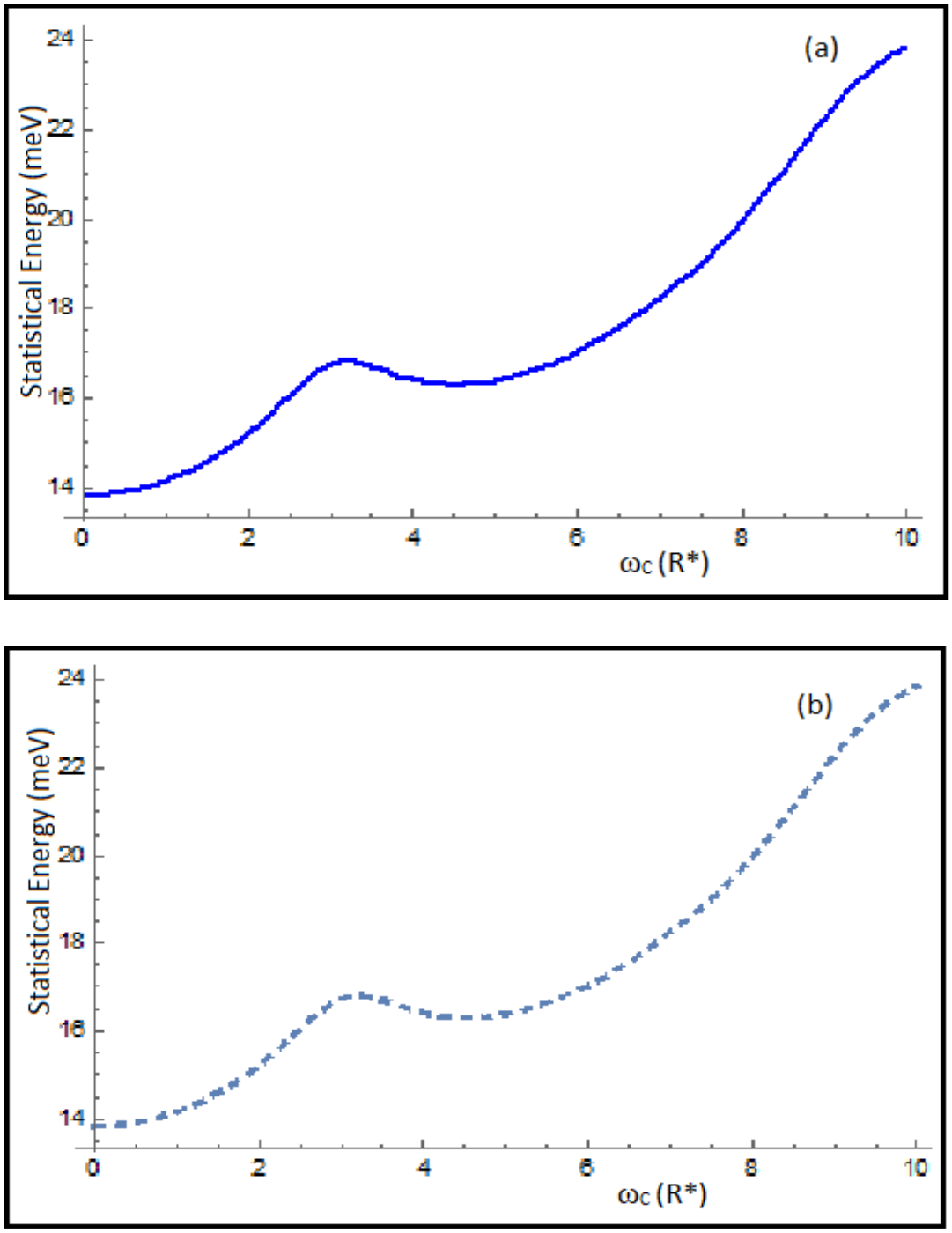

Figure (3.14): The statistical energy as a function of the magnetic field strength ω_c , at: $\eta=2R^*$, V_0=50 meV, T=10 K, R_0 =8 nm, for different quantum number. a) The radial quantum number n (0,2) and the angular quantum number m (-2,2). b) The radial quantum number n (0,4) and the angular quantum number m (-4,4).

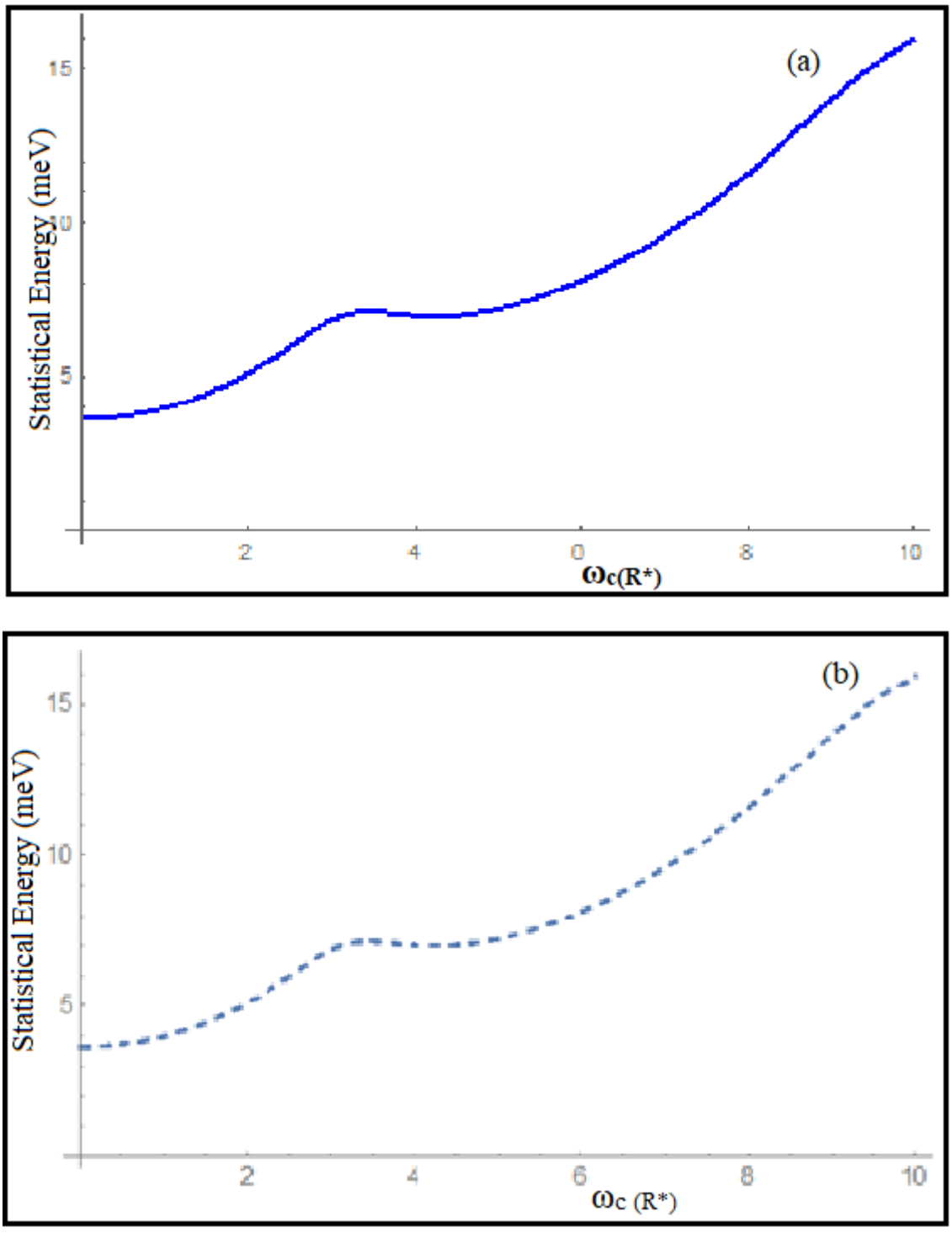

Figure (3.15): The statistical energy as a function of the magnetic field strength ω_c , at: $\eta=2R^*$, $V_0=30$ meV, T=10 K, R_0 =8 nm, for different quantum number. a) The radial quantum number n (0,2) and the angular quantum number m (-2,2). b) The radial quantum number n (0,4) and the angular quantum number m (-4,4).

After achieving a high convergence in the statistical energy, we turn now to calculate the magnetic quantities: magnetization (M) and susceptibility (χ) .

To obtain our required results for the magnetic properties of the QPD, we have presented our calculated statistical energy as shown in figure(3.16), figure(3.17) and figure(3.18) for different QPD physical parameters. The figures show the dependencies of the statistical energy on (ω_c) for different values of (η) and (V_0).

The effects of the η on the statistical energy is plotted in figure (3.16). The plot shows that for fixed value of the electric field, the statistical energy increases as the ω_c increases. It is clear that when the electric field strength gets higher the statistical energy gets lower for fixed magnetic field values.

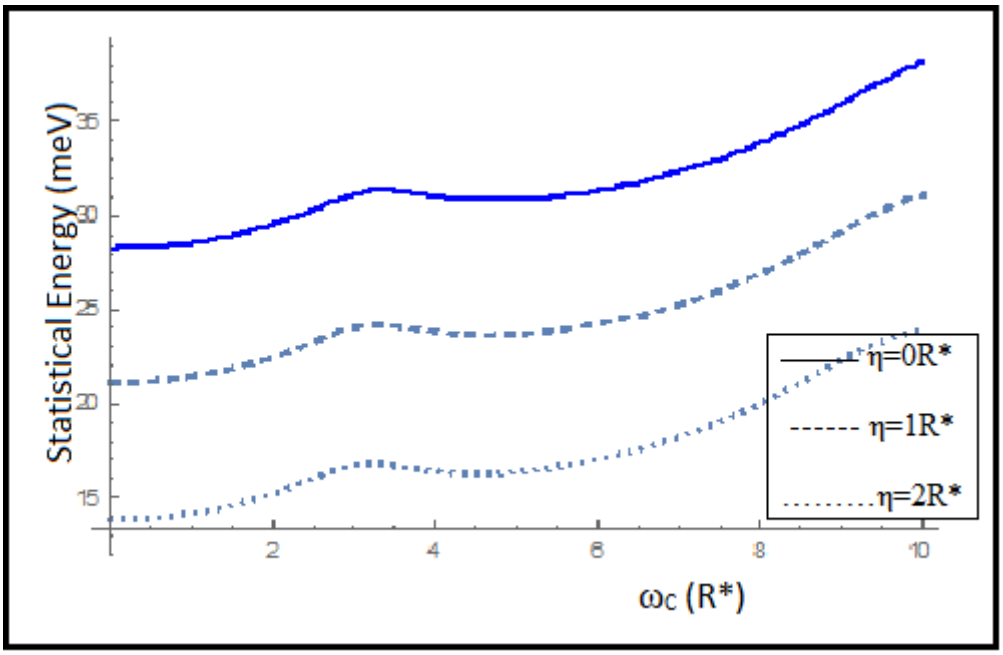

Figure (3.16): The statistical energy as a function of the magnetic field strength ω_c , at: R_0=8 nm, V_0=50 meV, T=10 K, for different values of η.

The effect of the zero points R_0 and the confinement potential V_0 on the statistical energy against the magnetic field strength is presented in figures (3.17) and (3.18), respectively. Figure (3.17) presents the variation of the statistical energy against R_0. The statistical energy increases as we decrease R_0, while ω_c is kept constant. Figure (3.18) shows the effect of the confinement potential V_0 on the statistical energy. As the confinement potential V_0 increases the statistical energy enhances.

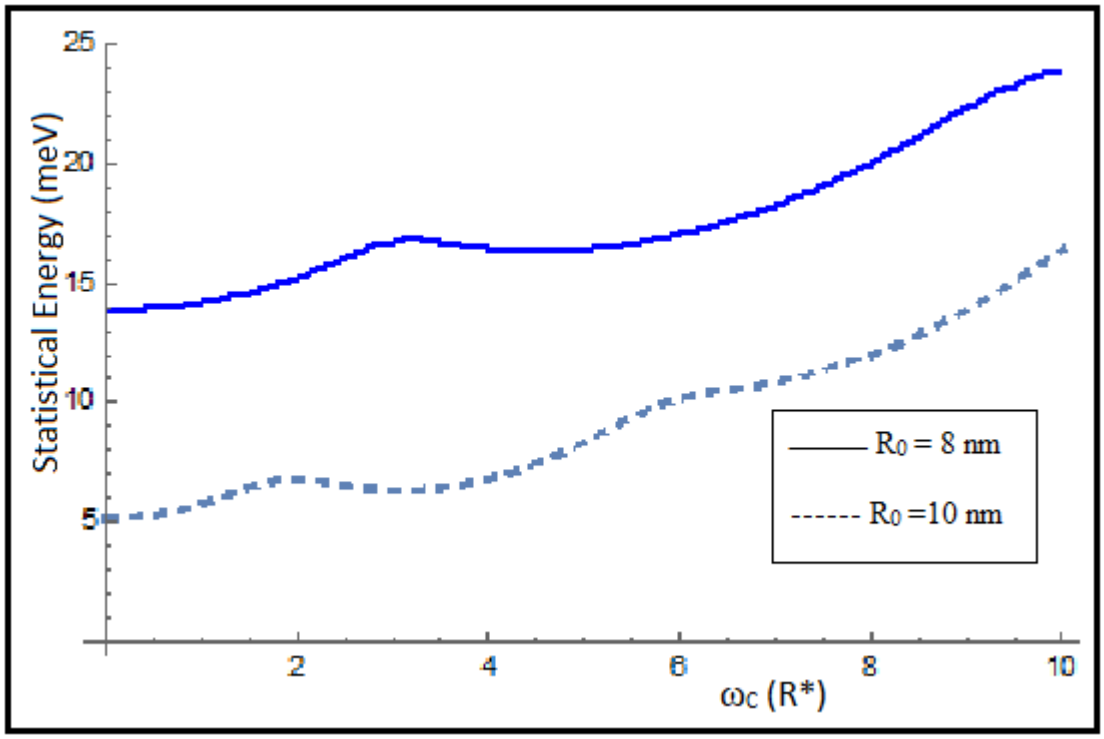

Figure (3.17): The statistical energy as a function of the magnetic field strength ω_c , at: $\eta=2R^*$, V_0=50 meV, T=10 K, for different values of R_0 .

To investigate the effect of the donor impurity on the statistical energy, we have plotted in figure (3.19), the statistical energy for zero and non-zero impurity cases. We can see the reduction in the statistical energy as we

include the impurity in the QPD due to its negative attractive energy in the QD Hamiltonians.

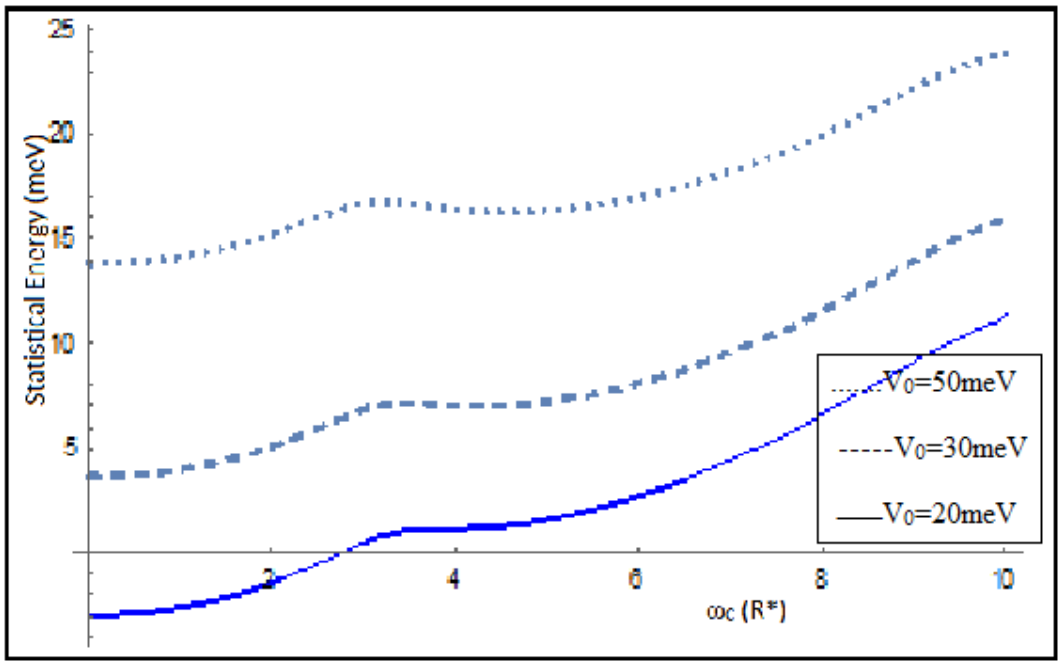

Figure (3.18): The statistical energy as a function of the magnetic field strength ω_c , at: R_0=8nm, η=2R*, T=10K, for different values of V_0 .

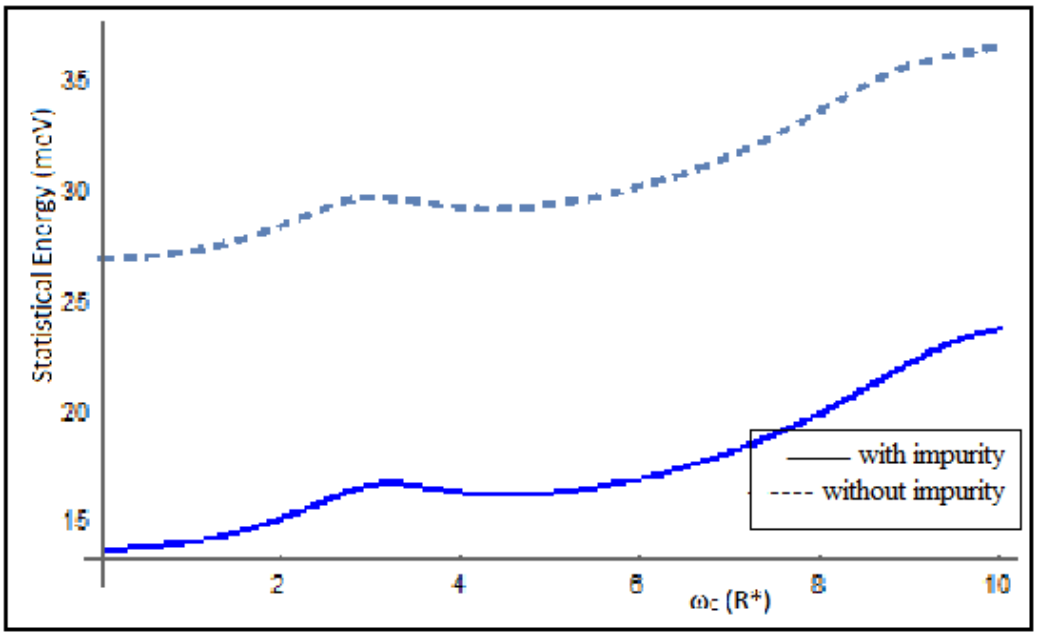

Figure (3.19): The statistical energy as a function of the magnetic field strength ω_c with (solid line)/ without (dashed line) impurity, at : R_0=8 nm, V_0=50 meV, η=2R*, T=10K.

3.4 Magnetization and Susceptibility

In this section, we present magnetization(M) and susceptibility (χ) of the QD as a function of different physical parameters. We calculate magnetization in unit of effective Bohr magneton $\mu_B = \frac{e\hbar}{2m*}$ =0.862 meV/T for GaAs.

Figures (3.20), (3.22), (3.24) and (3.26), show the magnetization behavior, as ω_c increases, the M decreases until it reaches a minimum value, after that it increases until reaches maximum value then it decreases again, this oscillating behavior is due to the QD energy level crossing crossings in figures (3.8) and (3.9). In figure (3.21), (3.23), (3.25) and (3.27) the curves clearly show that two magnetic phase transition; diamagnetic to paramagnetic and then to diamagnetic, at low magnetic field where the susceptibility is negative, and in this case the system is diamagnetic. As the ω_c increases the χ becomes positive, where the system turns to paramagnetic type.

The influence of absence or presence of the impurity on the M and χ appears in figure (3.20) and (3.21), respectively.

Figure (3.20) shows that the height of the peak is reduced and shifted towards a strong magnetic field value due to the donor of impurity which lowers the statistical energy in figure (3.19). Figure (3.20.a) and (3.20.b), show the behavior of the QD magnetization for different values of low V_0 = 10 meV and high V_0 = 50 meV, while the rest of the parameters are

kept unchanged. We can observe that the sign of M for V_0 = 10 meV is negative for all ω_c range, while M changes it sign from negative to positive and again to negative for the same ω_c range for high confining potential V_0 = 50 meV. In addition, the peaks are high and coincide and shifted to the right, high magnetic field, for V_0 = 50 meV, while they appear as two small separated ones for V_0 = 10 meV. For low confinement, V_0 = 10 meV, the impurity has a clear significant effect on M spectra. The impurity, with its negative energy contribution, shifted the peaks towards a high magnetic field range.

Figure (3.21.a) show that as the confinement potential V_0 loweres (V_0 = 10 meV), the effects of the donor impurity on the magnetic susceptibility the height of the peaks lowers and shifted to higher magnetic field value, and the peak are small when the magnetic field stronger, we note that at ω_c = 0, the presence of the impurity decreases the amplitude of the magnetic susceptibility. In figure (3.21.b) show that as the confinement potential V_0 increases (from 10 meV to 50 meV), at ω_c=0, the magnetic susceptibility nearly is equals, and the first peak almost overlapped high , whereas as magnetic field stronger the peak is separated and becomes small.

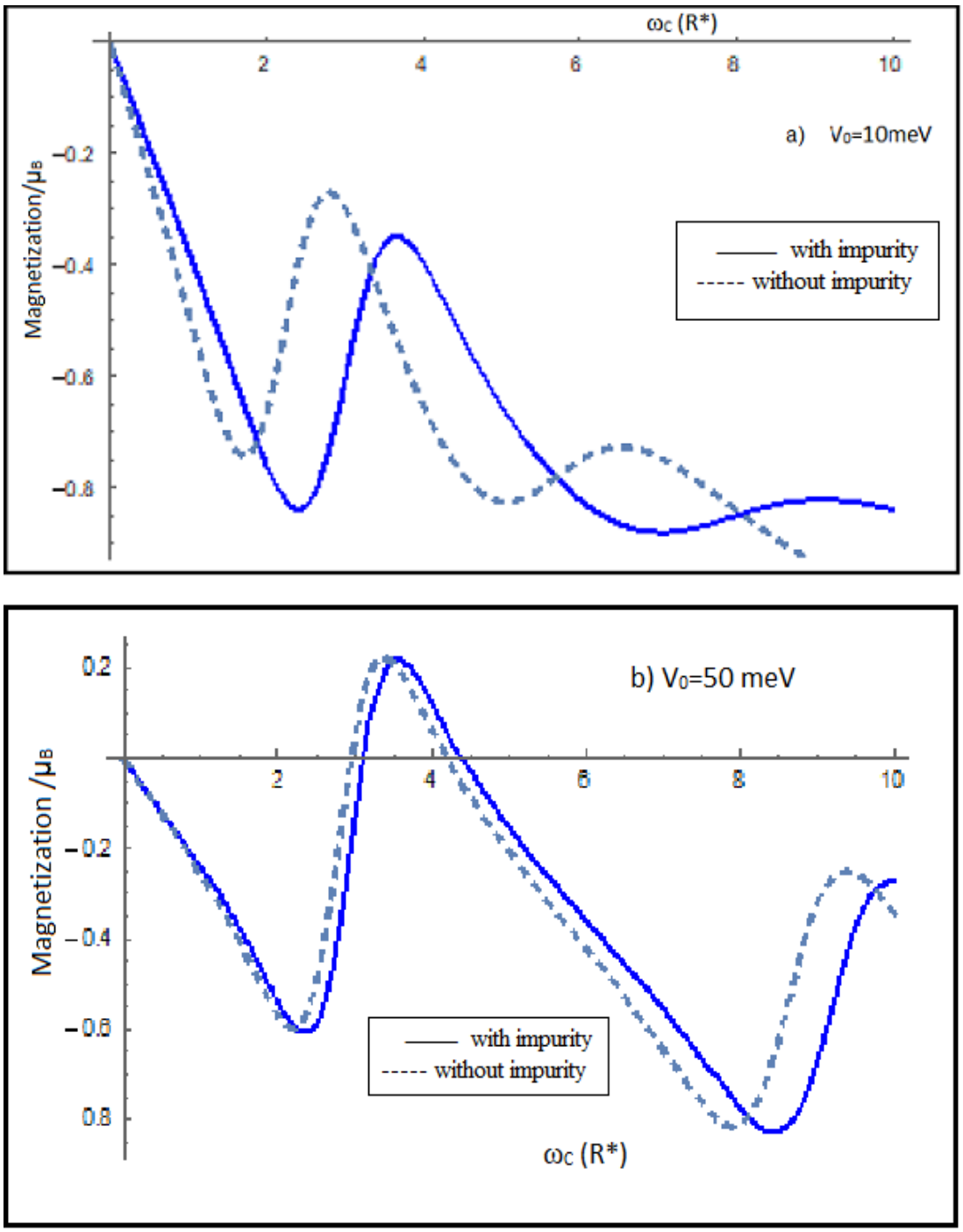

Figure(3.20): The magnetization M against the magnetic field strength ω_c with (solid line)/ without (dashed line) impurity, at R_0=8nm, T=10K, η=3R*, a) V_0=10 meV, b) V_0=50 meV.

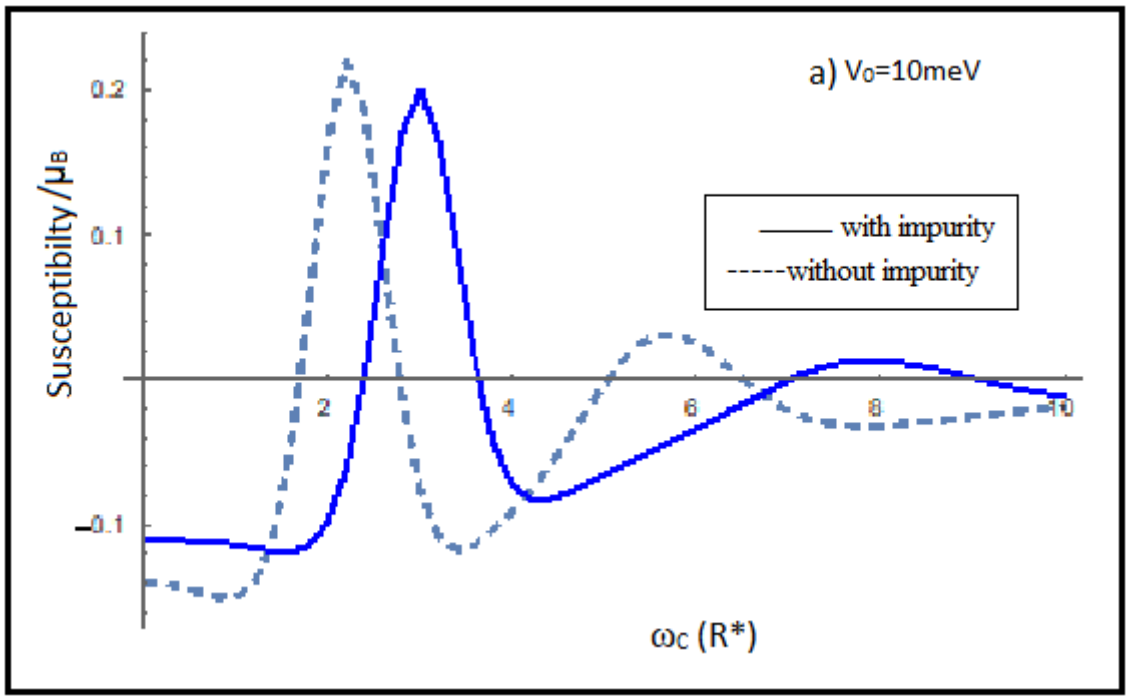

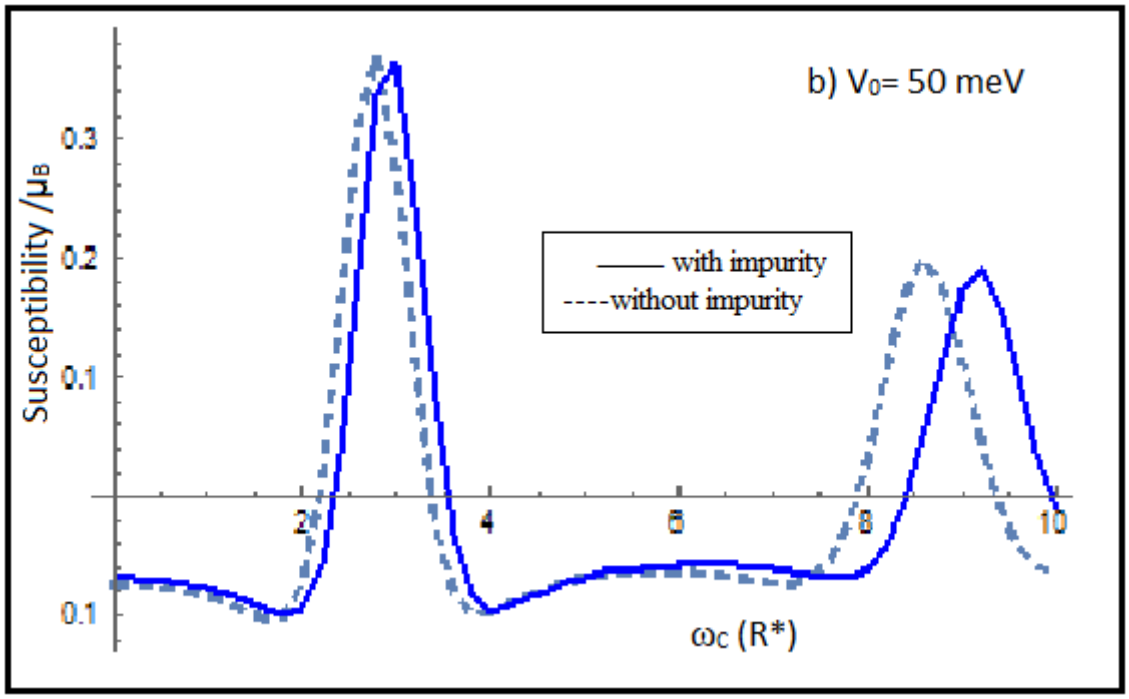

Figure(3.21): The susceptibility χ against the magnetic field strength ω_c with (solid line)/ without (dashed line) impurity, at R_0=8nm, T=10K, η=3R*, a) V_0= 10 meV, b) V_0= 50 meV.

In figure (3.22.a) and (3.22.b), we have shown the variation of the magnetization of the QD with the electric field strength (η=3R* and η= 5R). For low confinement potential (V_0=10 meV), the electric field shifts the two well separated peaks to left side, low magnetic field strength, and the magnetization is negative always. However, the peaks are coincide at high confinement, V_0=50 meV, and the magnetization has oscillating signs. The electric field turns the sign of the magnetization.

Figure (3.23) reflects the effect of the electric field on the magnetic susceptibility. From figure (3.23.a), for low value of the confinement potential V_0 (V_0= 10 meV), as the electric field strength (η) increases the height of peak is small and shifted to a lower magnetic field strength (ω_c). Whereas, the magnetic field strength (ω_c) is stronger the peak is small and large separated, at ω_c =0, the amplitude of the magnetic susceptibility increases as the electric field increase. In figure (3.23.b), as the confinement potential V_0 increases (V_0=5 0 meV), the influence of the electric field becomes small, and at ω_c =0, the magnetic susceptibilities nearly are equal. The first two peaks are coincide, while the second peaks is separated as the electric field changes.

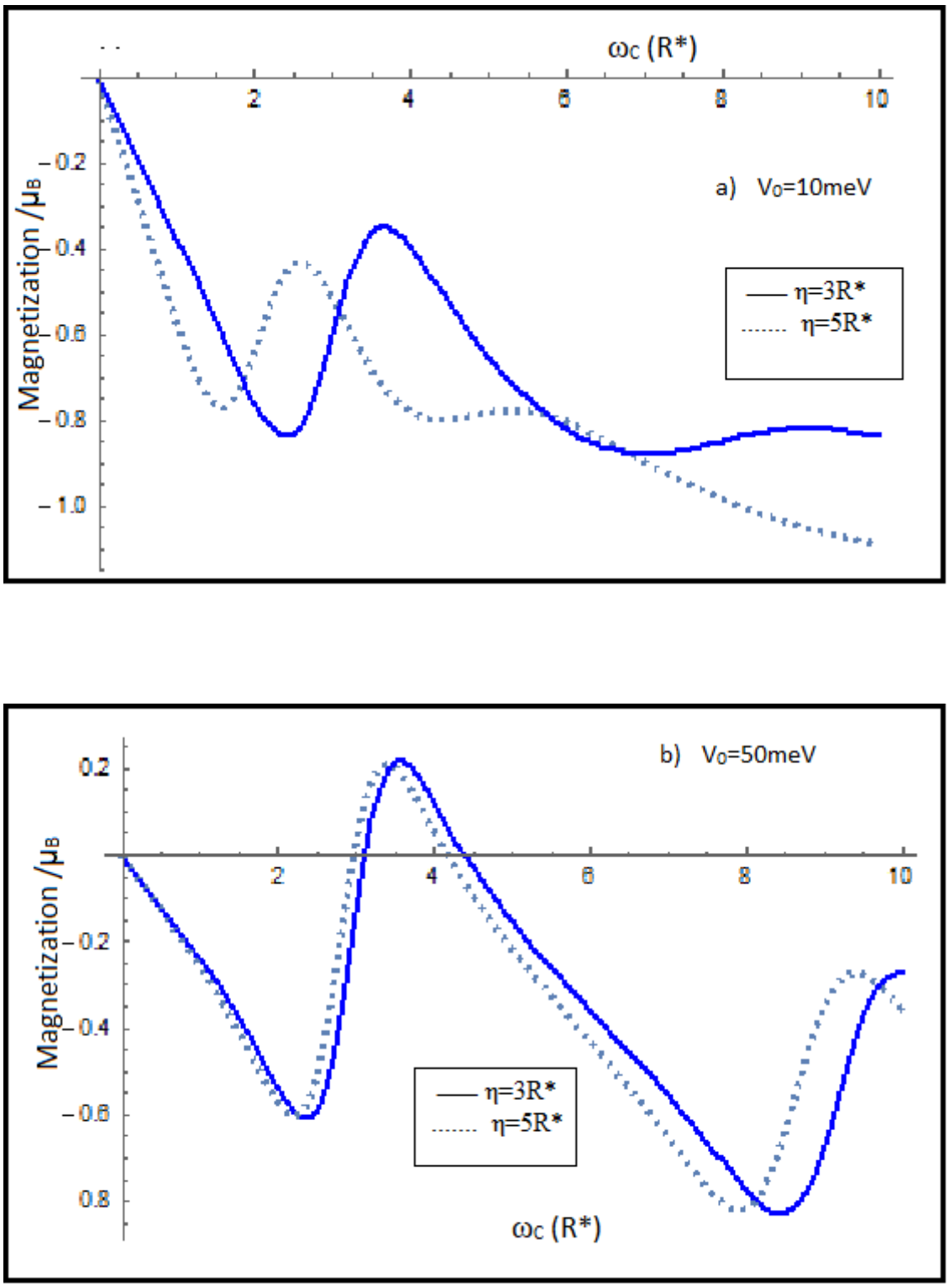

Figure (3.22): The magnetization M against the magnetic field strength ω_c , at R_0=8nm, T=10K, and various electric field strength η, a) V_0= 10 meV, b) V_0= 50 meV.

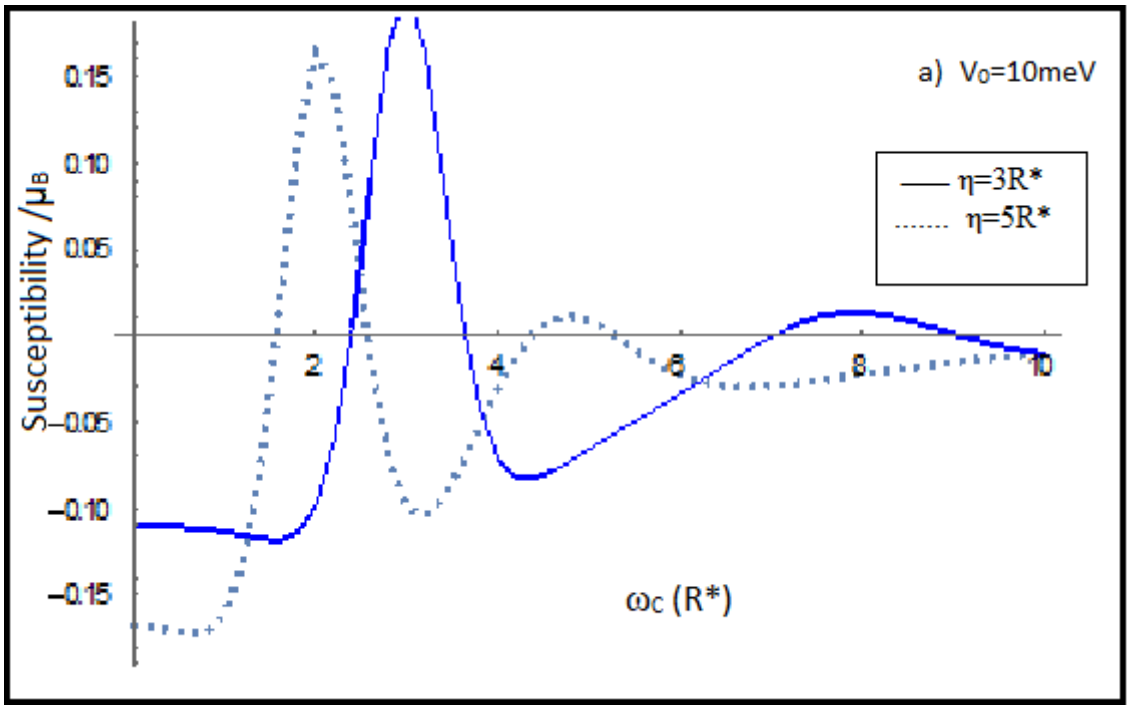

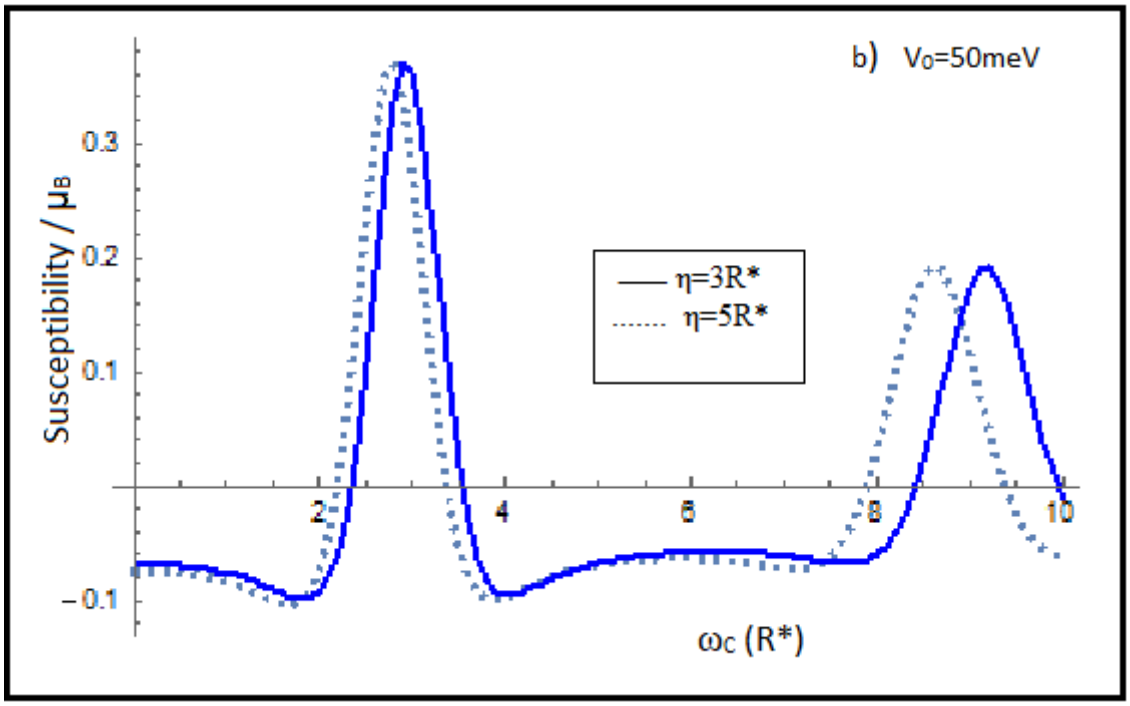

Figure(3.23): The susceptibility χ against the magnetic field strength ω_c , at R_0=8nm, V_0=10meV, T=10K, and various electric field strength η, a) V_0= 10 meV, b) V_0= 50 meV.

Figure (3.24) displays the effects of the potential strength V_0 on the magnetization, the magnetization curves show that, the height of the peak increases as the potential strength V_0 increases.

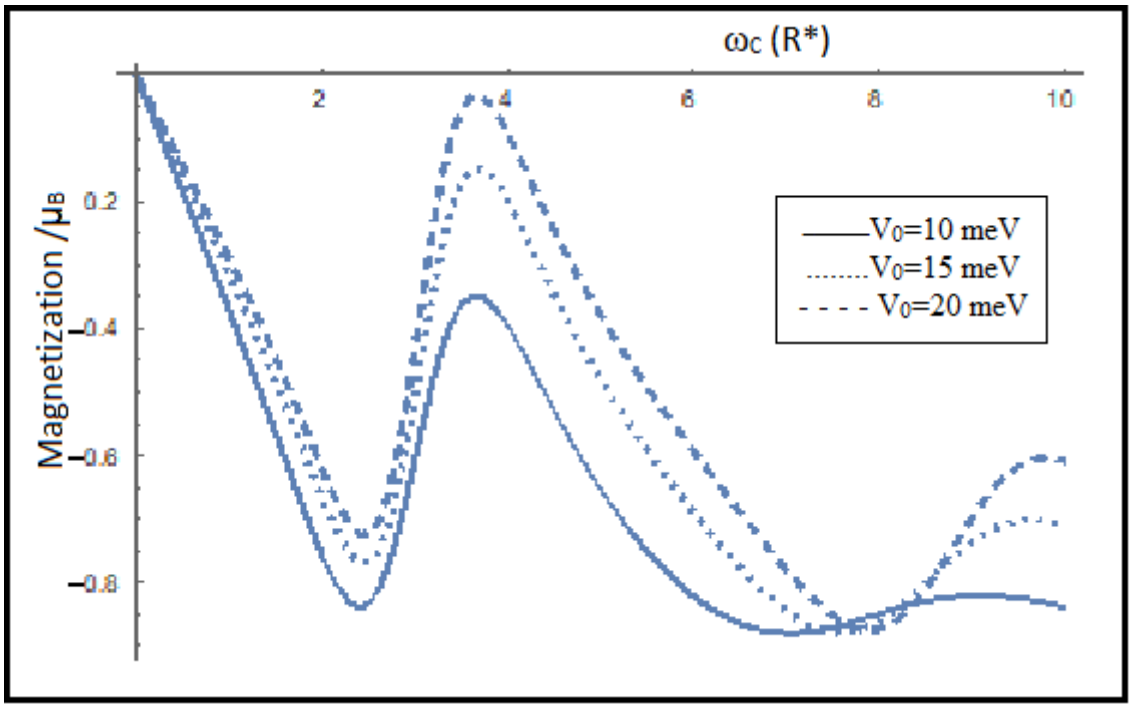

Figure (3.24): The magnetization M against the magnetic field strength ω_c , at R_0=8nm, T=10K, η=3R*,with different values V_0.

Figure (3.25) shows the effects of the potential strength V_0 on the susceptibility, as the potential strength V_0 increase the high of peaks increases. The small peak is shifted toward a high magnetic field strength as V_0 enhances.

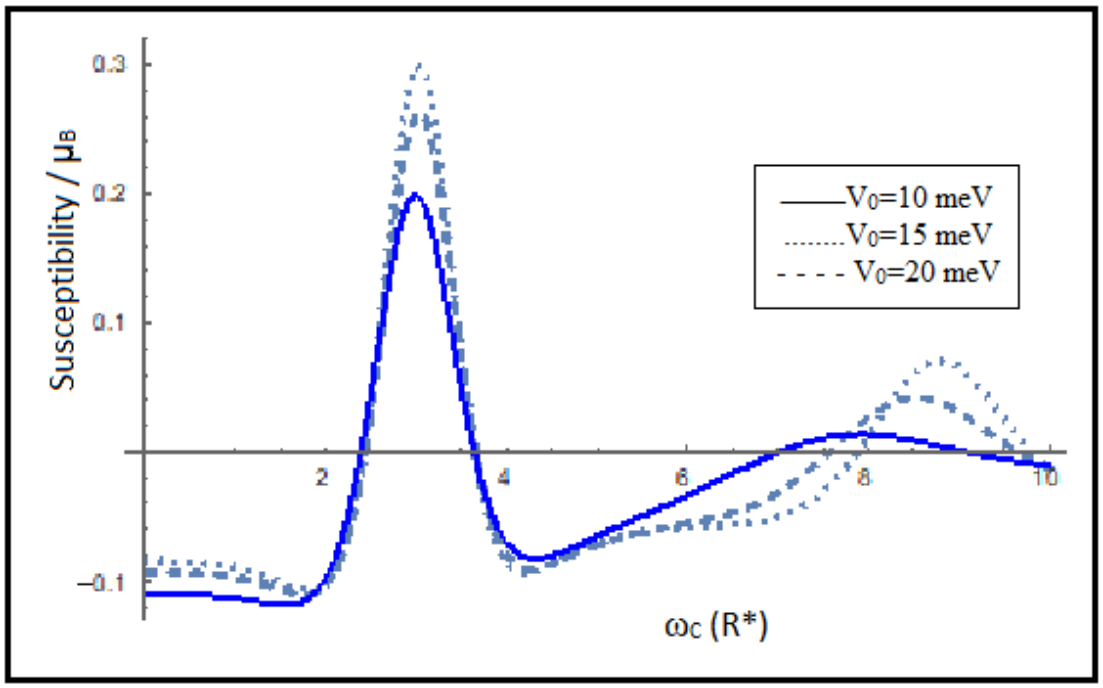

Figure(3.25): The susceptibility χ against the magnetic field strength ω_c , at R_0=8nm, T=10K, η=3R*, with different values V_0 .

Figure (3.26.a) and (3.26.b), shows the effect of the zero points (R_0) distance on the magnetization curves for V_0= 10 meV and V_0= 50 meV. For low confinement potential (V_0= 10 meV). Figure (3.26.a) shows a rapid oscillations and the peak shifts to low magnetic field range at high R_0 value (R_0 = 10nm), and the magnetization is negative for all magnetic field range. However, the sign of magnetization oscillates for high confinement potential and different zero points R_0.

Figure (3.27.a) and (3.27.b), show the effects of the zero points (R_0) on the susceptibility curves. As R_0 increases, the susceptibility curves shows more rapid oscillations, and at ω_c=0, the separation in susceptibility values increases for low confinement potential (V_0 = 10 meV), figure (3.27.a). For high confinement potential (V_0 = 50 meV), figure (3.27.b), the second

peaks becomes more well separated and susceptibility values has small variation at ω_c=0.

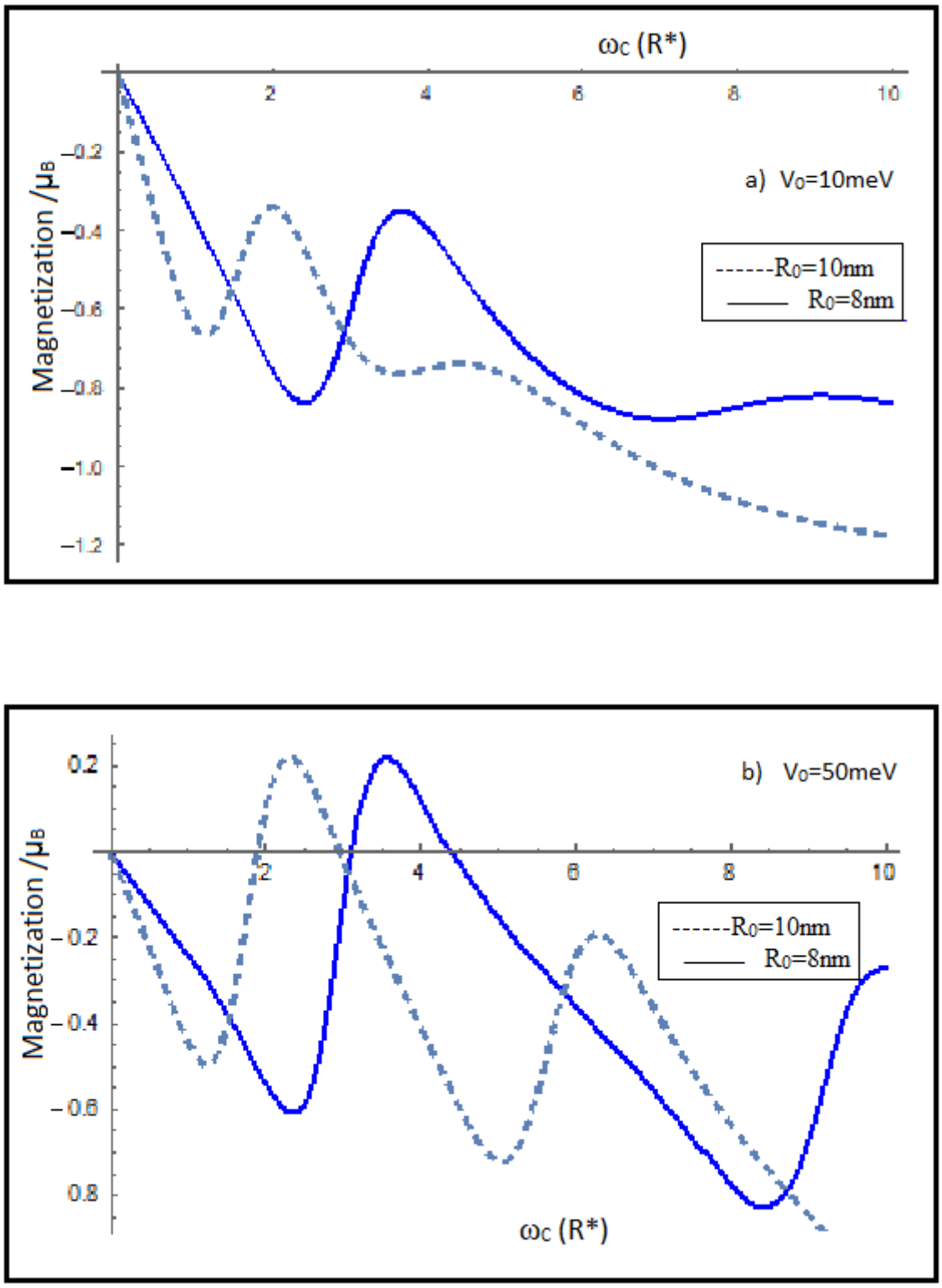

Figure(3.26): The magnetization M against the magnetic field strength ω_c , at V_0=10meV, T=10K, η=3R*, for different values R_0 , a) V_0= 10 meV, b) V_0= 50 meV.

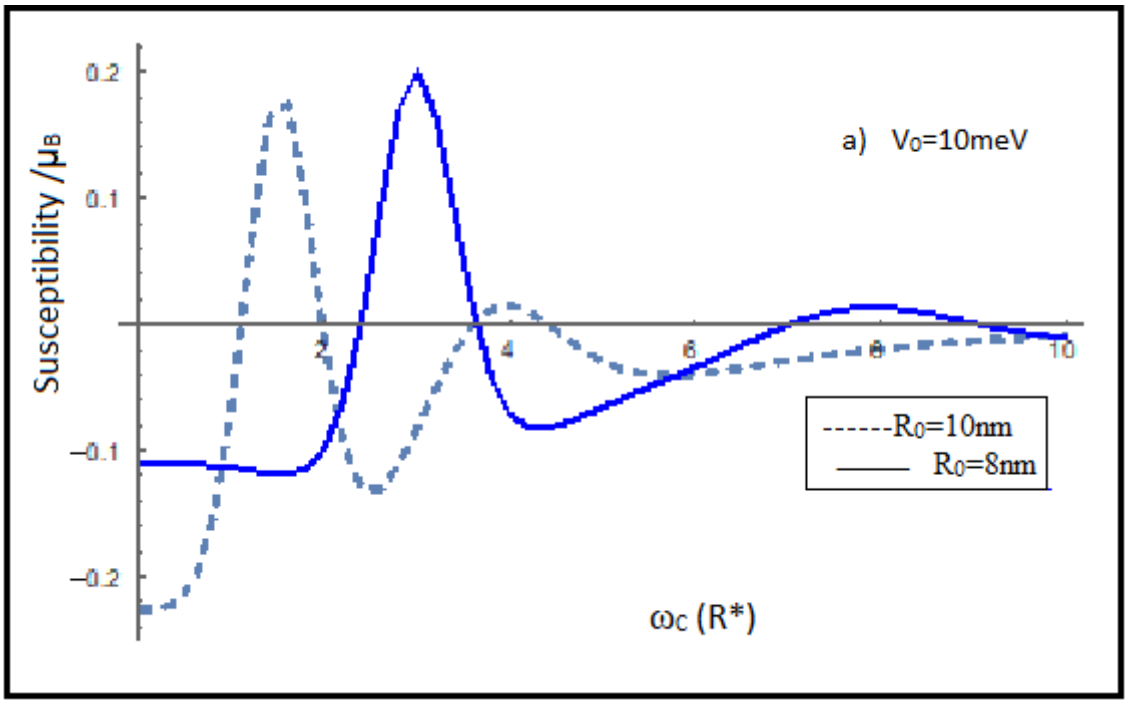

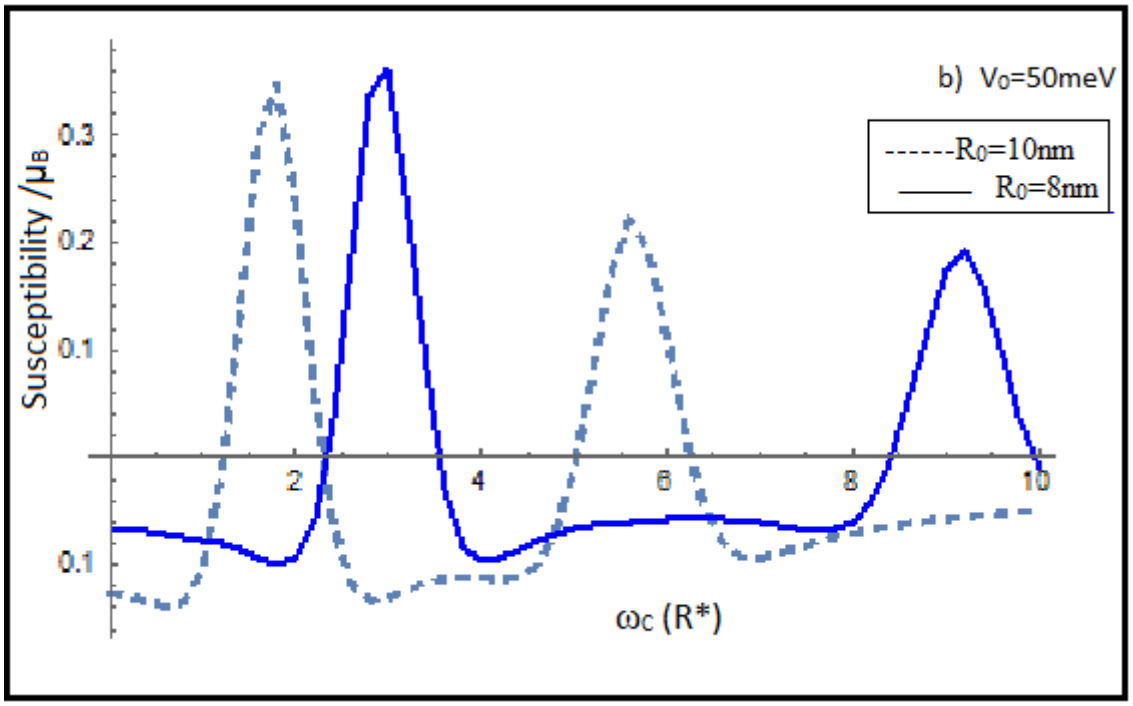

Figure (3.27): The susceptibility χ against the magnetic field strength ω_c , at V_0=10meV, T=10K, η=3R*,for different values R_0 .

The effects of the temperature on the magnetization of the QPD is shown in figure (3.28.a) and (3.28.b). As the temperature increases the hight of peaks are reduced and shifted towards a high magnetic field value, for low confinement potential (V_0= 10 meV), figure (3.28.a), the magnetization is negative also. However, for high confinement potential (V_0= 50 meV), figure (3.28.b), the sign of magnetizations oscillates between negative and positive.

In figure (3.29.a) and (3.29.b), we have displayed the effect of the temperature on the susceptibility similar to magnetization curves. The figures show significant changes in the behavior of the susceptibility for different confinements potential. For V_0 =10 meV, the first peak is high and the second peak is low. This order is reversed for high confinement, (V_0 =50 meV).

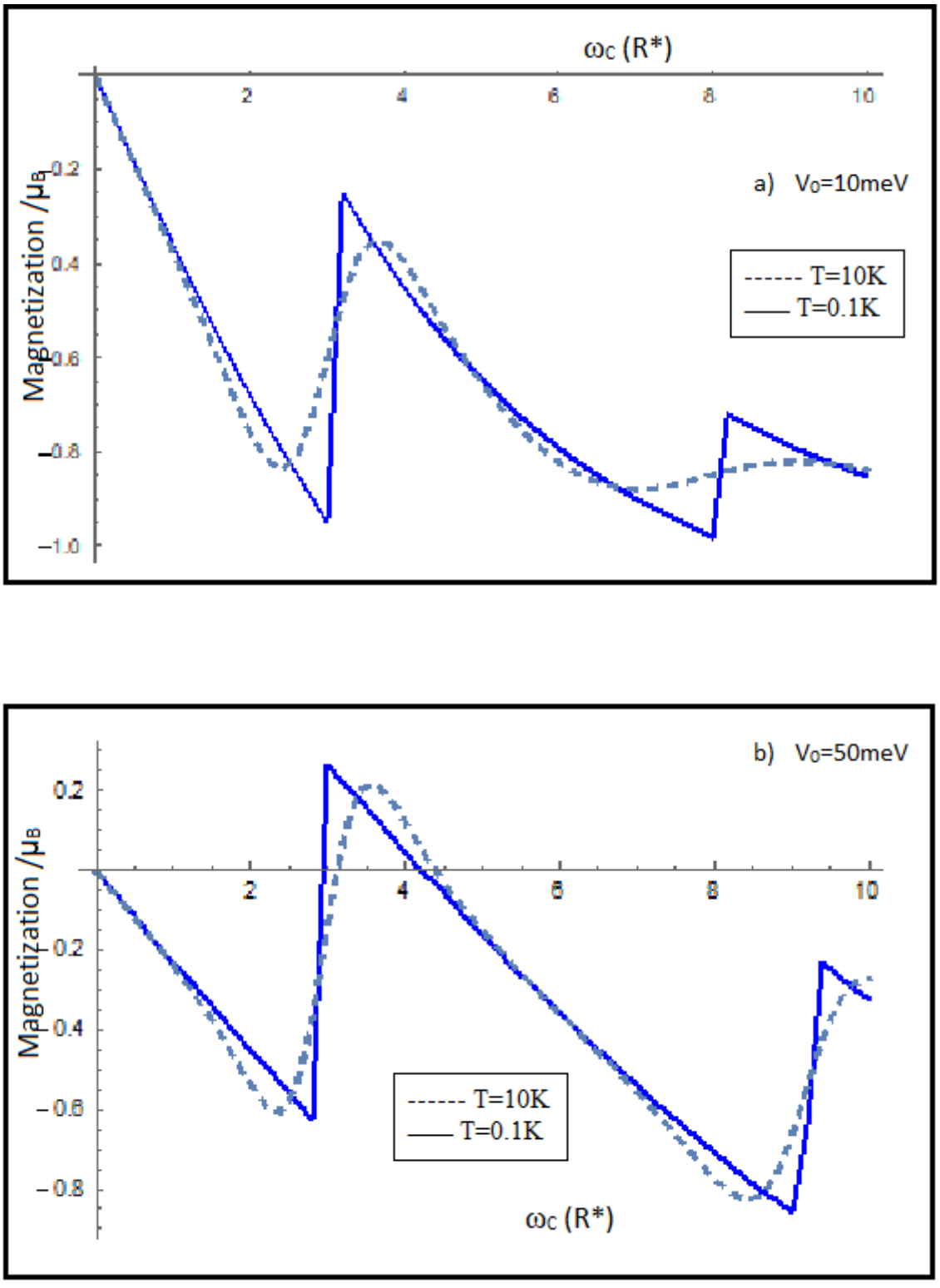

Figure (3.28): The magnetization M against the magnetic field strength ω_c , at V_0=10meV, R_0=8nm, η=3R*, for different values T, a) V_0= 10 meV, b) V_0= 50 meV.

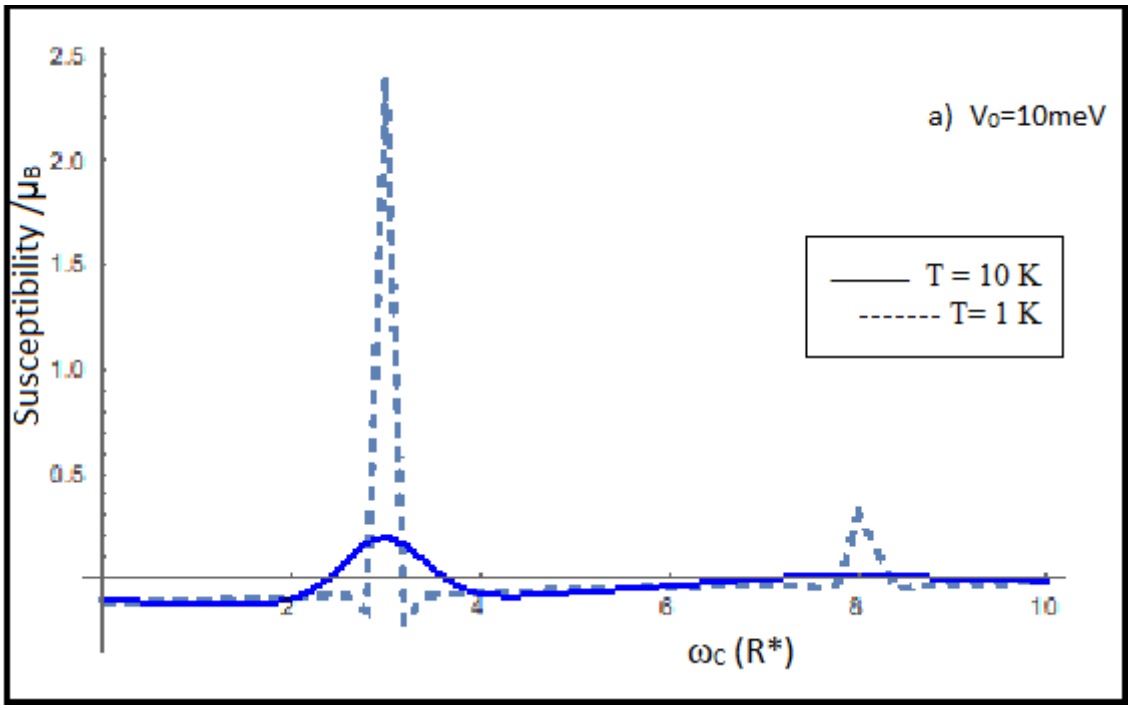

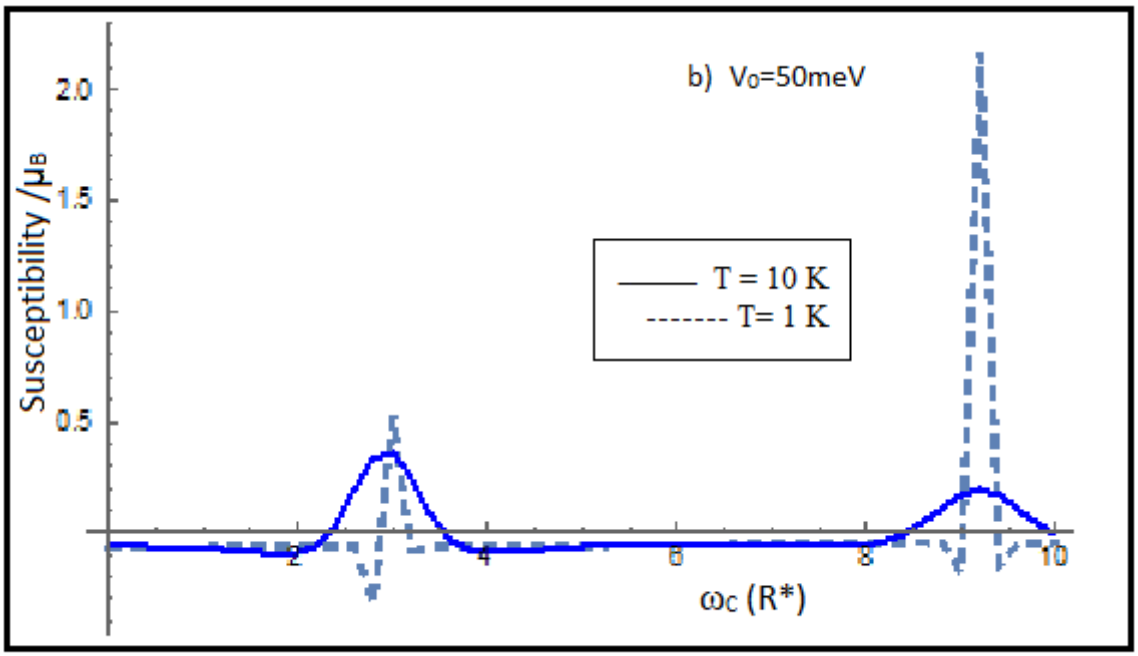

Figure (3.29): The susceptibility χ against the magnetic field strength ω_c , at V_0=10meV, R_0=8nm, η=3R*,for different values T, a) V_0= 10 meV, b) V_0= 50 meV.

Chapter Four
Conclusions

In this work, we have studied the effects of electric and magnetic fields and temperature on magnetic properties of the QPD in the presence of donor impurity. Using the shifted 1/N expansion method, we have calculated the energy eigenvalue of the ground state and low lying state as a function of different physical parameters; magnetic field strength ω_c, electric field strength η, the potential confinement R_0 ,V_0 and the presence or absence of impurity. Our results show that the magnetic field strength ω_c , electric field strength η, the potential confinement R_0 ,V_0 and the donor impurity have great effects on the average statistical energy and binding energy. The presence of the impurity and increasing in η and R_0 reduces in the average energy and binding energy. While, the increasing in V_0 and ω_c enhancement of the average energy and binding energy. In addition, we have displayed the dependence of magnetization and magnetic susceptibility of donor impurity in QPD with various physical parameters (ω_c, η, T, R_0 , V_0).

In summary, the statistical energy, magnetization and magnetic susceptibility show an oscillating behavior due to the energy level crossing of the QPD. It is found that as we increase the electric, magnetic fields it varies the values of the statistical energy , which in turn effects on magnetization and susceptibility curves of the QPD. The GaAs QPD material shows a magnetic phase transition, from diamagnetic to

paramagnetic type, under the influence of the magnetic and electric applied fields.

References

[1] Jun Mao, Zihang Liu & Zhifeng Ren, **Size effect in thermoelectric materials,** (2016).

[2] Bimberg, D. and Pohl, U.W., **Quantum dots: promises and accomplishments.** Materials Today, **14**(9), pp.388-397, (2011).

[3] R. Khordad, Hydrogenic Impurity States in Quantum Psedudot: ***Spin-Orbit Interaction, Relativistic Correction, and Diamagnetic Susceptibility***, **Int J Theor Phys**, **52**: 837-848,(2013).

[4] R. Khordad, Physica E: **Bound polaron in a quantum psedudot under Rashba effect,** Low-dimensional Systems and Nanostructures, **69**, 249-252, (2015).

[5] NF. Johnson, ***Quantum dots: few-body, low-dimensional systems***, **Journal of Physics**, Condensed Matter, 7, 6,(1995).

[6] www.sp.phy.**cam.ac.uk/research/fundamentals-of-low-dimensional-semiconductor-systems/antid,** semiconductor physics group-university of Cambridge.

[7] J. M. Elzerman, Ronald Hanson, L. P. **Kouwenhoven, Semiconductor few-electron quantum dots as spin qubits**, Quantum Computing in Solid State Systems, pp 298-305, (2006).

[8] C. Bose C.K. Sarkar, **Binding Energy of Impurity States in Spherical GaAs–Ga1–xAlxAs Quantum Dots,** physica status solid,Volume218, Issue2, Pages 461-469, (2000).

[9] O. Bayrak I. Boztosun H. Ciftci, ***Exact analytical solutions to the Kratzer potential by the asymptotic iteration method, Wiley Periodicals, Inc.*** **Int J Quantum Chem,** Volume107, Issue3, Pages 540-544, (2007).

[10] A. Dehyar, G. Rezaei and A. Zamani, **Electronic structure of a spherical quantum dot:Effects of the Kratzer potential, hydrogenic impurity,external electric and magnetic fields**, Physica E **84**, 175-181, (2016).

[11] G. Rezaei, S. Shojaeian Kish, **Effects of external electric and magnetic fields, hydrostatic pressure and temperature on the binding energy of a hydrogenic impurity confined in a two-dimensional quantum dot**, Physica E **45**, 56-60, (2012).

[12] G. Rezaei, N.A. Doostimotlagh, **External electric field, hydrostatic pressure and conduction band non-parabolicity effects on the binding energy and the diamagnetic susceptibility of a hydrogenic impurity quantum dot,** Physica E **44**, 833-838, (2012).

[13] G. Rezaei, S.F. Taghizadeh, A.A. **Enshaeian, External electric field, hydrostatic pressure and temperature effects on the binding energy of an off-center hydrogenic impurity confined in a spherical Gaussian quantum dot,** Physica E **44**, 1562-1566, (2012).

[14] Jian-Hui Xuan, Chao Liu, **Binding energy of an off-center hydrogenic donor in a spherical quantum dot with strong parabolic confinement**, Physica E **41**, 41-44, (2008).

[15] Oktay Aydogdu, Ramadan Sever, **Solution of the Dirac equation pseudoharmonic potential by using the Nikiforov- Uvarov method**, Phys. Scr. **80**, (2009).

[16] R. Khordad, ***Confinement of an exciton in a quantum dot: effect of modified Kratzer potential***, **Indian Journal of Physica**, **87**, Issue 7, 623-628, (2013).

[17] Bekir Çakır, Yusuf Yakar, Ayhan Ozmen, **Magnetic Field Effects on Oscillator Strength, Dipole Polarizability and Refractive Index Changes in Spherical Quantum Dot**, Chemical Physics Letters, **684**, 250-256, (2018).

[18] D.B. Hayrapetyan, S.M. Amirkhanyan, E.M. Kazaryan, H.A. Sarkisyan, **Effect of hydrostatic pressure on diamagnetic susceptibility of hydrogenic donor impurity in core/shell/shell spherical quantum dot with Kratzer confining potential,** Physica E: Low-Dimensional Systems and Nanostructures, **84**, 367-371,(2016).

[19] D.Sanjeev Kumar, Soma Mukhopadhyay, ***Ashok Chatterjee, Magnetization and susceptibility of a parabolic InAs quantum dot with electron–electron and spin–orbit interactions in the presence of a magnetic field at finite temperature***, **Journal of Magnetism and Magnetic Materials, 418,** 169–174, (2016).

[20] M. Akbari G. Rezaei R. **Khordad, Rashba and Dresselhaus spin-orbit interactions effects on electronic features of a two dimensional elliptic quantum dot,** Superlattices and Microstructures, **101**, 429-435, (2017).

[21] E.Hijaz and M.K.Elsaid, ***The electronic states and magnetization of coupled AlGaAs/GaAs quantum dots in magnetic fields,*** **International Journal of Modern Physics B32**, 1850011 (2017).

[22] M.K.Elsaid and E.Hijaz, **Magnetic Susceptibility of Coupled Double GaAs Quantum Dot in Magnetic Fields**. Acta Physica Polonica **A131** ,6 (2017).

[23] E.Hijaz, M.K.Elsaid and M.Elhasan, ***Magnetization of Coupled Double Quantum Dot in Magnetic Fields,*** **Journal of Computational and Theoretica Nanoscience 14** ,1700-1705 (2017).

[24] A.Shaer, M.K.Elsaid and M.Elhasan, ***The magnetic properties of a quantum dot in a magnetic field,*** **Turkish Journal of Physics 40**,209 (2016).

[25] M.Elsaid, Physica B: **Effects of applied magnetic field on the energy levels of shallow donors in a parabolic quantum dot**, Condensed Matter **202**, 202-206, (1994).

[26] M.Elsaid, **The ground-state energy of an exciton in a parabolic quantum dot**, Semicond. Sci. and Technol. **9**,272 (1994).

[27] M.El-Said, **Ground-state properties of quantum dots with a magnetic field,** physica Status solidi (b) **193**, 105-111, (1996).

[28] A. Shaer, M.K. Elsaid and M. Elhasan, ***Magnetization of GaAs Parabolic Quantum Dot by Variation Method*, Journal of Physical Science and Application 6**, 39-46, (2016).

[29] F. Bzour, A .Shaer, M.K. Elsaid, ***The effects of pressure and temperature on the exchange energy of a parabolic quantum dot under a magnetic field,*** **Journal of Taibah University for Science 11,** 1122-1134, (2017).

[30] F. Bzour, M.K. Elsaid, A. Shaer, **The Effects of Pressure and Temperature on the Magnetic Susceptibility of Semiconductor Quantum Dot in A Magnetic Field,** Applied Physics Research **9**, 77,(2017).

[31] A. Çetin, **A quantum pseudodot system with a two-dimensional pseudoharmonic potential**, Physics Letters A **372,** 3852–3856, (2008).

[32] Wenfang Xie n, ShijunLiang, **Optical properties of a donor impurity in a two-dimensional quantum pseudodot**, Physica B: **406,** 4657–4660, (2011).

[33] Alaeddin SayahianJahromi , G.Rezaei**, Electromagnetically induced transparency in a two-dimensional quantum pseudo-dot system: Effects of geometrical size and external magnetic field,** Physica B: **456**, 103–107, (2015).

[34] Sameer M.Ikhdair a, Majid Hamzavi, **A quantum pseudodot system with two-dimensional pseudoharmonic oscillator in external magnetic and Aharonov-Bohm fields,** Physica B: **407**, 4198–4207, (2012).

[35] O.S.Bauzha, O.M.Voskoboynikov, O.V.Tretyak, O.S.Sinyavskij, **Magnetic properties of quantum rings in the presence of spin orbit interaction**, Physics of nanosystems, **51**, 9, (2006).

[36] Abdurahman Cetin, Yunus Sakar, ***Quantum Pseudodot Systems in One-Dimension, Two-Dimensions and Three-Dimensions,*** **International Journal of Natural and Engineering Sciences 10**: 42-46, (2016).

[37] M.El-Said, M.A. Saa, ***The Energy Spectra of GaAs/AlxGa1-xAs Quantum Dots,*** **Turkish Journal of Physics 22**, 885-894, (1998).

[38] T. Imbo, A. Pagnamenta, and U.Sukhatme, **Bound States of the Yukawa Potential via the Shifted 1/N Expansion Technique**. Physics Letters A, 105, 183-187, (1984).

جامعة النجاح الوطنية

كلية الدراسات العليا

الخصائص المغناطيسية لشائبة مانحة في نقطة كمية شبه موصل من مادة (GaAS)

إعداد

هناء محمد ريحان

إشراف

أ.د. محمد السعيد

قدمت هذه الأطروحة استكمالاً لمتطلبات الحصول على درجة الماجستير في الفيزياء، بكلية الدراسات العليا، في جامعة النجاح الوطنية، نابلس- فلسطين.

2019

الخصائص المغناطيسية لشائبة مانحة في نقطة كمية شبه موصل من مادة (GaAS)

إعداد

هناء محمد ريحان

إشراف

أ.د. محمد السعيد

الملخص

تم دراسة الخواص المغناطيسية مثل التمغنط والقابلية المغناطيسية لشائبة مانحة في نقطة كمية شبه موصل بوجود المجالات المغناطيسية والكهربائية، باستخدام طريقة مفكوك 1 / N تم حل دالة هاملتون لحساب الطاقة لعدة مستويات بدلالة متغيرات فيزيائية. أظهرت نتائج حساب الطاقة لشائبة مانحة في نقطة كمية شبه موصل توافقا جيدا مقارنة بنتائج مماثلة منشورة. والمتغيرات فيزيائية هي: وجود الشوائب، شدة المجالين المغناطيسي والكهربائي، وقوة حصر الالكترون. تأثير المتغيرات الفيزيائية بدا واضحاً على كل من: طاقة الربط ومعدل الطاقة وعلى الخواص المغناطيسية التمغنط والقابلية المغناطيسية، حيث تظهر منحنيات هذه الخواص سلوكا متذبذبا يعزى إلى تقاطع مستوى الطاقة.